

AD-A052 265

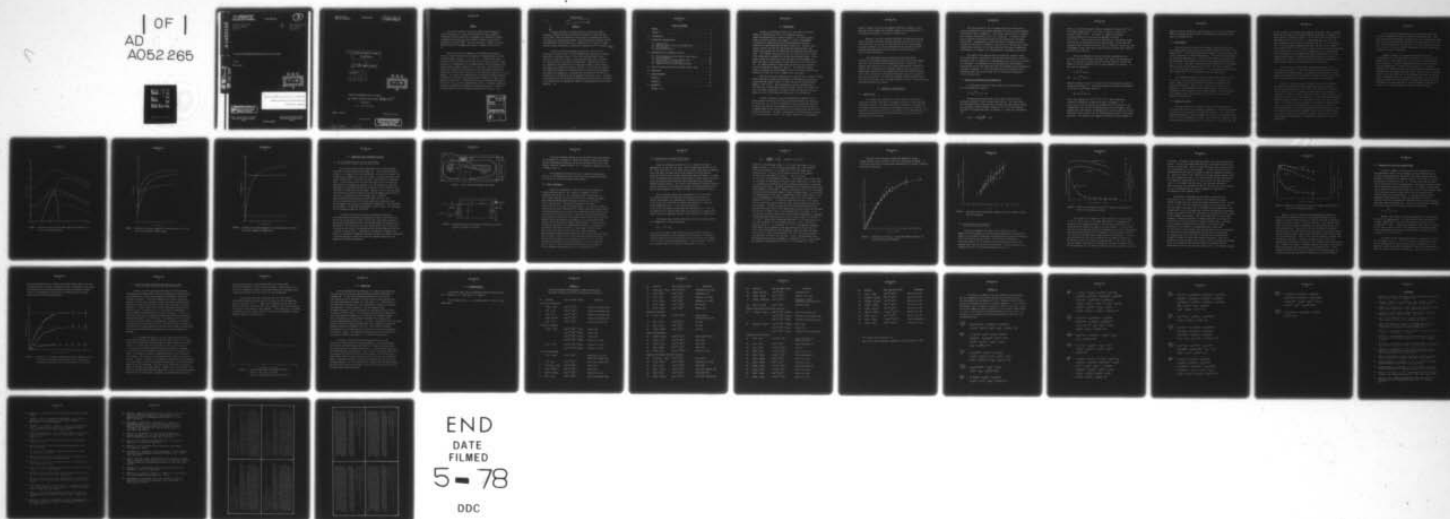
DEFENCE RESEARCH ESTABLISHMENT VALCARTIER (QUEBEC)  
A SEALED HIGH-REPETITION-RATE TEA-CO<sub>2</sub> LASER, (U)  
MAR 78 P PACE, M LACOMBE  
DREV-R-4092/78

F/G 20/5

UNCLASSIFIED

NL

1 OF 1  
AD  
A052 265



NTIS REPRODUCTION  
BY PERMISSION OF  
INFORMATION CANADA

UNCLASSIFIED

3

CRDV RAPPORT 4092/78  
DOSSIER: 3633H-001  
MARS 1978

DREV REPORT 4092/78  
FILE: 3633H-001  
MARCH 1978

AD A 052265

A SEALED HIGH-REPETITION-RATE TEA-CO<sub>2</sub> LASER

P. Pace

M. Lacombe

AD No. 1  
DDC FILE COPY

DDC  
RECEIVED  
APR 5 1978  
B

Centre de Recherches pour la Défense  
Defence Research Establishment  
Valcartier, Québec

DISTRIBUTION STATEMENT A  
Approved for public release;  
Distribution Unlimited

BUREAU - RECHERCHE ET DEVELOPPEMENT  
MINISTRE DE LA DEFENSE NATIONALE  
CANADA

RESEARCH AND DEVELOPMENT BRANCH  
DEPARTMENT OF NATIONAL DEFENCE  
CANADA

NON CLASSIFIÉ

CRDV R-4092/78  
DOSSIER: 3633H-001

UNCLASSIFIED

14 DREV-R-4092/78  
FILE: 3633H-001

6 A SEALED HIGH-REPETITION-RATE  
TEA-CO<sub>2</sub> LASER.

by

10 P. Pace and M. Lacombe

11 Mar 78

12 47P.

DDC  
RECEIVED  
APR 5 1978  
B

CENTRE DE RECHERCHES POUR LA DEFENSE

→ DEFENCE RESEARCH ESTABLISHMENT 404945

VALCARTIER

Tel: (418) 844-4271

Québec, Canada

March/mars 1978

NON CLASSIFIE

DISTRIBUTION STATEMENT A  
Approved for public release;  
Distribution Unlimited

404 945

JOB

## UNCLASSIFIED

i

RESUME

Nous avons construit un laser  $\text{CO}_2$  TEA à double décharge de petites dimensions et l'avons fait fonctionner à cadence moyenne. L'addition de petites quantités d'hydrogène et de monoxyde de carbone au mélange gazeux  $\text{He-CO}_2\text{-N}_2$  nous a permis d'obtenir plus de  $2 \times 10^6$  impulsions en circuit fermé. Dans ces conditions, l'énergie de sortie atteint environ 250 mJ/impulsion lorsque la cadence est de 40 à 50 Hz.

Dans le but de mieux comprendre les différents processus en jeu dans un laser scellé, nous avons analysé le mélange gazeux à l'aide d'un spectromètre de masse. A la suite de ces analyses, nous avons trouvé qu'il est possible de faire fonctionner un laser en circuit fermé pourvu que la concentration de l'oxygène présente dans le mélange gazeux  $\text{He-CO}_2\text{-N}_2\text{-CO-H}_2$  demeure inférieure à 1-2 pour cent. Nous avons ensuite comparé nos résultats aux prédictions tirées d'un modèle théorique qui tient compte des processus mettant en jeu les particules neutres et les ions négatifs. Ces calculs nous montrent que la présence de faibles quantités d'oxygène et d'eau dans le milieu gazeux fait augmenter le nombre d'ions négatifs produits dans la décharge au point que le rapport ions négatifs à électrons,  $N_n/N_e$ , peut se rapprocher de l'unité. Le modèle indique également que des quantités adéquates d'hydrogène/deutérium et de monoxyde de carbone peuvent servir à contrôler la dissociation du  $\text{CO}_2$ . (NC).

ACCESSION for	
NTIS	White Section <input checked="" type="checkbox"/>
DDC	Buff Section <input type="checkbox"/>
UNANNOUNCED	<input type="checkbox"/>
JUSTIFICATION _____	
BY _____	
DISTRIBUTION/AVAILABILITY CODES	
Dist.	AVAIL. and/or SPECIAL
A	



UNCLASSIFIED

ii

TEN TO THE 6TH POWER

ABSTRACT

A compact atmospheric pressure  $\text{CO}_2$  laser utilizing a double-discharge technique has been constructed and operated at moderate repetition rates. With the addition of small amounts of hydrogen and carbon monoxide to the  $\text{He-CO}_2\text{-N}_2$  gas mixture, sealed operational lifetimes exceeding  $2 \times 10^6$  pulses have been obtained. Operating in this mode, the output energy is about 250 mJ/pulse at repetition frequencies of 40-50 pulses/s.

In order to better understand the processes involved in the operation of a sealed laser, we have performed mass spectroscopic measurements of the laser gas mixture. It has been determined that sealed operation is possible as long as oxygen concentration below 1-2 percent in a  $\text{He-CO}_2\text{-N}_2\text{-CO-H}_2$  gas mixture is maintained. Experimental results are compared to the predictions of a theoretical model in which neutral and negative-ion processes have been included. The calculations indicate that, when small amounts of oxygen or water are present in the discharge, the negative-ion population is significantly increased and the ratio of negative-ions to electrons  $N_n/N_e$  can approach values near unity. The model also predicts that the dissociation equilibrium of the  $\text{CO}_2$  can be controlled by the addition of the appropriate amounts of hydrogen/deuterium and carbon monoxide. (U).

## UNCLASSIFIED

iii

TABLE OF CONTENTS

RESUME . . . . .	i
ABSTRACT . . . . .	ii
1.0 INTRODUCTION . . . . .	1
2.0 THEORETICAL CONSIDERATIONS . . . . .	2
2.1 Negative Ions . . . . .	2
2.2 Molecular Dissociation and Recombination . . . . .	3
2.3 The Discharge . . . . .	5
2.4 Negative-Ion Results . . . . .	5
3.0 COMPARISON WITH EXPERIMENTAL RESULTS . . . . .	11
3.1 The High-Repetition-Rate TEA-CO <sub>2</sub> Laser Design . . . . .	11
3.2 Laser Performance . . . . .	13
3.3 Dissociation in a Sealed TEA-CO <sub>2</sub> Laser . . . . .	14
3.4 Sealed TEA-CO <sub>2</sub> Laser Operation . . . . .	17
3.5 Comparison with the Rate Equation Model . . . . .	21
4.0 LONG-LIFE SEALED HIGH-REPETITION-RATE TEA-CO <sub>2</sub> LASER . . . . .	23
5.0 CONCLUSIONS . . . . .	25
6.0 ACKNOWLEDGEMENTS . . . . .	26
APPENDIX A . . . . .	27
APPENDIX B . . . . .	31
7.0 REFERENCES . . . . .	35
FIGURES 1 to 11	

## 1.0 INTRODUCTION

Recently, considerable interest has been shown in the development of sealed TEA-CO<sub>2</sub> lasers [1,2] operating at pulse repetition frequencies up to about 2 pulses/s. For certain applications of interest, notably laser radars, it would be advantageous to increase the repetition rate while maintaining the desirable qualities of sealed operation and small overall size. However, calculations indicate [3] that, for high-repetition-rate operation, the volume of gas between the electrodes must be renewed at least twice per pulse. This imposes restrictions on the size of the device as a sufficient volume must be provided for the gas recirculation system. In the present design this problem has been overcome by the development of a small wind-tunnel system capable of flow velocities of the order of 20 m/s. The double-discharge system chosen for the laser was the dielectrically encapsulated trigger bar type [4]. The electrode configuration, the design and the performance of this laser have been described previously [5] and will only be summarized in this report.

When this system was operated with a 'make-up' flow of about 15 l/min, steady operation at repetition frequencies of 100 pulses/s was possible giving multimode output energies of about 300 mJ/pulse and peak powers around 1.5 MW in 80 ns. When operating in a sealed configuration we have been able to obtain more than  $2 \times 10^6$  pulses; however, the output energy in this mode of operation is reduced to about 250 mJ/pulse with peak powers of about 1 MW at repetition frequencies of 30-40 pulses/s.

In order to obtain a long sealed operational lifetime, H<sub>2</sub> and CO were added to the basic He-N<sub>2</sub>-CO<sub>2</sub> gas mixture following the techniques of Stark et al [1]. During the experiments, mass-spectroscopic analysis of various gas mixtures was performed and the results were correlated to a computer model of the chemical processes occurring during and after the electrical discharge. The model is based upon the work presented by Shields et al [2] and Davies et al [6]. This model, along with the experimental



results, combine to show how the gaseous dissociation products of the He-N<sub>2</sub>-CO<sub>2</sub> mixture change the discharge negative-ion concentration so as to permit the transition to arcing in a sealed laser.

Moreover, since the principal difficulty in obtaining long-term sealed operation is ensuring that the reactions involved do not lead to the irreversible loss of CO<sub>2</sub>, we have included the reactions proposed by Smith and Browne [7] for the reformation of the CO<sub>2</sub> from the carbon monoxide and oxygen which form as a result of the dissociation of CO<sub>2</sub> by electron collisions.

The experimental results indicate that long-term sealed operation can be obtained provided that the oxygen concentration remains less than 1-2% and that the CO<sub>2</sub> decomposition can be controlled. The computer model indicates that 1-2% of added oxygen greatly increases the negative-ion concentration (the dominant negative-ion being CO<sub>4</sub><sup>-</sup> for 2% added oxygen) and that the CO<sub>2</sub> decomposition (and thus oxygen concentration) can be controlled by the addition of small amounts of H<sub>2</sub> and CO to the initial gas mixture. This work was performed at DREV between September 1976 and June 1977 under PCN 33H01 (formerly PCN 34A01) "Double-Discharge High-Repetition-Rate CO<sub>2</sub> Lasers".

## 2.0 THEORETICAL CONSIDERATIONS

### 2.1 Negative Ions

The negative ions produced in a glow discharge initially arise either from two-body dissociative attachment reactions or from three-body attachment reactions. The model describes the attachment, detachment and ion-molecule reactions occurring in an atmospheric-pressure discharge. It also takes into account the positive-ion-negative-ion recombination, the dissociation of neutral species by electron-molecule collisions and some molecule-molecule reactions.

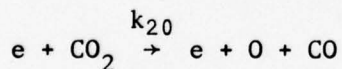


The initial negative ions are created either by two-body dissociative attachment or by three-body attachment reactions; the most important of these are listed in Appendix A. They include reactions with the largest rate constants involving  $\text{CO}_2$ ,  $\text{CO}$ ,  $\text{O}$ ,  $\text{O}_2$ ,  $\text{H}_2$  and  $\text{H}_2\text{O}$ . It should be noted that no reactions involving the oxides of nitrogen have been considered in the model. Experimentally we have been unable to measure any concentrations of the oxides of nitrogen to a sensitivity of 100 ppm and at these concentrations Shields et al [2] have shown that they make no significant contribution to the negative-ion concentrations at atmospheric pressures.

The negative ions undergo various ion-molecule reactions along with various neutral constituents, both two-body and three-body. The loss of negative ions is assumed to be a homogeneous process and no wall reactions are considered. The homogeneous losses considered are the detachment reactions and the two- and three-body positive-ion-negative-ion recombination presented in Appendix A. Values for these positive-ion-negative-ion recombination rates are not well known but the rates given by Shields et al [2] have been used.

## 2.2 Molecular Dissociation and Recombination

In a  $\text{He-N}_2\text{-CO}_2$  mixture the major source of  $\text{CO}_2$  dissociation is the electron-molecule reaction:

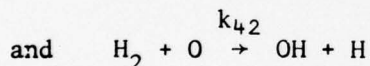
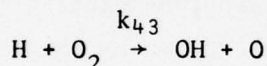


The dissociation coefficient  $\alpha/P$  for this reaction has been measured in Section 3.3 for a typical laser mixture. Its value varies with the energy density injected into the laser, but under typical operating conditions a value of about  $6 \text{ electron}^{-1} \text{ cm}^{-1} \text{ torr}^{-1}$  was obtained. This will be discussed more fully in Section 3.3. Using the relationship [2]:

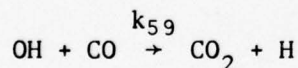
$$(\alpha/P) = \frac{3.6 \times 10^{16}}{v_d} \quad (\text{k})$$

where  $v_d$  is the electron drift velocity (assumed to be about  $3 \times 10^6$  cm s<sup>-1</sup> for an E/N of about  $2 \times 10^{-16}$  V cm<sup>2</sup>, [8], we obtain a value of  $k$  to be about  $0.5 \times 10^{-9}$  cm<sup>3</sup>s<sup>-1</sup>. This value is roughly in agreement with that of Smith and Austin [9] who obtained a value of  $1 \times 10^{-9}$  cm<sup>3</sup>s<sup>-1</sup>. Since N<sub>2</sub> and CO are dissociated at a considerably slower rate than CO<sub>2</sub> we assume that they are undissociated. We also make the assumption that the dissociation rate of O<sub>2</sub> is similar to that of CO<sub>2</sub>, that of hydrogen is about four times as great and that of water about twice as great as that of CO<sub>2</sub> [2].

Several recombination reactions have been incorporated into the model, the most important being those that effect the reformation of CO<sub>2</sub>. In our analysis we have used the reactions proposed by Smith and Browne [7] for the reformation of CO<sub>2</sub> using hydrogen as a catalyst. In this case the reactions:



would be expected to occur. The value for the rate constant  $k_{43}$  will be discussed in Section 3.5. The fastest reaction involving the reformation of CO<sub>2</sub> from the OH radical would be:



with a rate constant of  $1.5 \times 10^{-13}$  cm<sup>3</sup>s<sup>-1</sup> [7]. Other significant reactions involving the OH radical are given in Appendix A. It can be seen by these reactions that hydrogen acts as a catalyst in the reformation of CO<sub>2</sub> from the discharge products of CO and oxygen. This suggests that small amounts of hydrogen and CO could be added to the laser gas mixture to try and bias the CO<sub>2</sub> decomposition reaction in the reverse direction. The equations also suggest the addition of small amounts of

oxygen to help the formation of the OH radical, but, as will be shown, the addition of oxygen greatly increases the negative-ion concentration and leads to discharge arcing.

### 2.3 The Discharge

The electrical excitation for the model is provided in the form of a Gaussian pulse with a total area of  $3 \times 10^6$  electrons  $\text{cm}^{-3}\text{s}$  with a mean energy of 1 eV. A full-width-half-maximum (FWHM) of 300 ns was used to most closely approximate the actual pumping pulse. The total area of the pulse was determined experimentally. It was the value necessary to produce the measured amount of decomposition per pulse in a standard mixture of  $\text{He:N}_2:\text{CO}_2 = 70:15:15$ . The value so obtained of  $3 \times 10^6$  electrons  $\text{cm}^{-3}\text{s}$  corresponds with the value given by Shields et al [2] for a TEA laser discharge of 0.5 nF (at 25 kV) per  $\text{cm}^2$  of electrode. It is also assumed that the field,  $E/N$ , is about  $2 \times 10^{-16}$  V- $\text{cm}^2$  and does not vary with gas mixture.

The differential equations for the eleven neutral species ( $\text{H}$ ,  $\text{H}_2$ ,  $\text{CO}$ ,  $\text{O}$ ,  $\text{O}_2$ ,  $\text{O}_3$ ,  $\text{CO}_2$ ,  $\text{H}_2\text{O}$ ,  $\text{OH}$ ,  $\text{HO}_2$  and  $\text{H}_2\text{O}_2$ ) and the six negative-ion species ( $\text{CO}_3^-$ ,  $\text{O}^-$ ,  $\text{O}_2^-$ ,  $\text{CO}_4^-$ ,  $\text{OH}^-$  and  $\text{H}^-$ ) were solved iteratively using a Runge-Kutta technique. The full set of equations is presented in Appendix B. The development of other neutral species ( $\text{He}$ ,  $\text{N}_2$ ) is not considered as their populations are assumed constant. We have also made the assumption that charge neutrality is preserved to a high degree within the discharge [6].

### 2.4 Negative-Ion Results

We first consider the situation in which the gaseous decomposition products have not had a chance to accumulate. This would correspond to the first few laser pulses of a newly filled laser. Fig. 1 shows the computed development of the main negative-ion species in a mixture of  $\text{He:N}_2:\text{CO}_2 = 70:15:15$  at atmospheric pressure. The main peak was found to be  $\text{CO}_3^-$  with other peaks involving  $\text{CO}_4^-$ ,  $\text{O}_2^-$ ,  $\text{O}^-$ ,  $\text{H}^-$  and  $\text{OH}^-$ . The peaks of  $\text{OH}^-$  and



$H^-$  are a result of an assumed water impurity of 100 ppm. The  $H^-$  is mainly formed by the dissociative attachment of  $H_2O$  and then  $OH^-$  is formed by two-body processes, reactions 30 and 35. The  $O^-$  comes from the dissociative attachment of  $CO_2$  but then reacts in a three-body process to form  $CO_3^-$  and, subsequently,  $O_2^-$  and  $CO_4^-$  by reactions 34 and 40. It can be seen from Fig. 1 that  $CO_3^-$  reaches a maximum after about 100-200 ns with a population of about  $5 \times 10^{11} \text{ cm}^{-3}$  which gives a negative-ion-to-electron concentration  $N_n/N_e$  of about 0.02 at the peak of the pumping pulse. In the afterglow of the discharge the total negative-ion population decays both by recombination and detachment. Individual peaks may continue to increase in magnitude for a short time because the ion-molecule processes produce the species faster than the ion-loss mechanisms can remove them.

In the case of a sealed laser the dissociation products will be allowed to accumulate. Thus after several pulses there will be small concentrations of oxygen and CO. The effects of these additives on the negative-ion populations can be studied by adding these gases to the laser mixture and calculating the effects on the negative-ion population.

Firstly, if molecular oxygen is added to the He- $N_2$ - $CO_2$  mixture the three-body attachment reaction becomes important in creating  $O_2^-$ . However this combines later in time with  $CO_2$  to form  $CO_4^-$  by reaction 40. For the addition of only 2% oxygen the total negative-ion population is increased by a factor of about 7 ( $CO_4^-$  now being the dominant negative ion) such that the ratio  $N_n/N_e$  is now about 0.3. If the oxygen concentration is further increased to about 10% it is found that the ratio  $N_n/N_e$  becomes about 1 (the values of  $N_n/N_e$  are quoted at the peak of the pumping pulse). Fig. 2 is a plot of the concentrations of  $CO_3^-$ ,  $CO_4^-$  and  $O_2^-$  (at their concentrations after 150 ns) for varying amounts of added oxygen. Again, the results shown are for the standard 70-15-15, He- $N_2$ - $CO_2$  gas mixture. It is obvious that the  $CO_4^-$  becomes the dominant peak and, also, that the total negative-ion population is considerably increased for about 1-2% added oxygen.



It was found that the addition of CO in quantities up to about 10% does not appreciably affect the negative-ion concentration. However, the addition of hydrogen, although it does not significantly change the  $\text{CO}_3^-$  and  $\text{CO}_4^-$  concentration, does lead to increased amounts of  $\text{H}^-$  and  $\text{OH}^-$ . Also the addition of water produces  $\text{H}^-$  as the dominant ion and as shown in Fig. 3, the total negative-ion population can be significantly increased for about 5% added  $\text{H}_2\text{O}$ .

Nighan and Wiegand [10] suggest that negative ions play an important role in the ionization instabilities in low-pressure gas dynamic lasers. They computed that in a CW  $\text{CO}_2\text{-N}_2\text{-He}$  laser the dominant ion species is  $\text{CO}_3^-$  and its population could be greater than the electron concentration. Several other authors [11, 12, 13] have indicated that similar processes occur in atmospheric-pressure molecular discharges and can produce discharge arcing. However, due to the rapid change in the rate coefficients with discharge conditions, one can not directly extrapolate from the low-pressure conditions, but one can conclude that addition of small amounts of oxygen significantly increases the negative-ion population and, as will be discussed in Section 3.3, a small (1-2%) oxygen concentration leads to discharge arcing.

UNCLASSIFIED

8

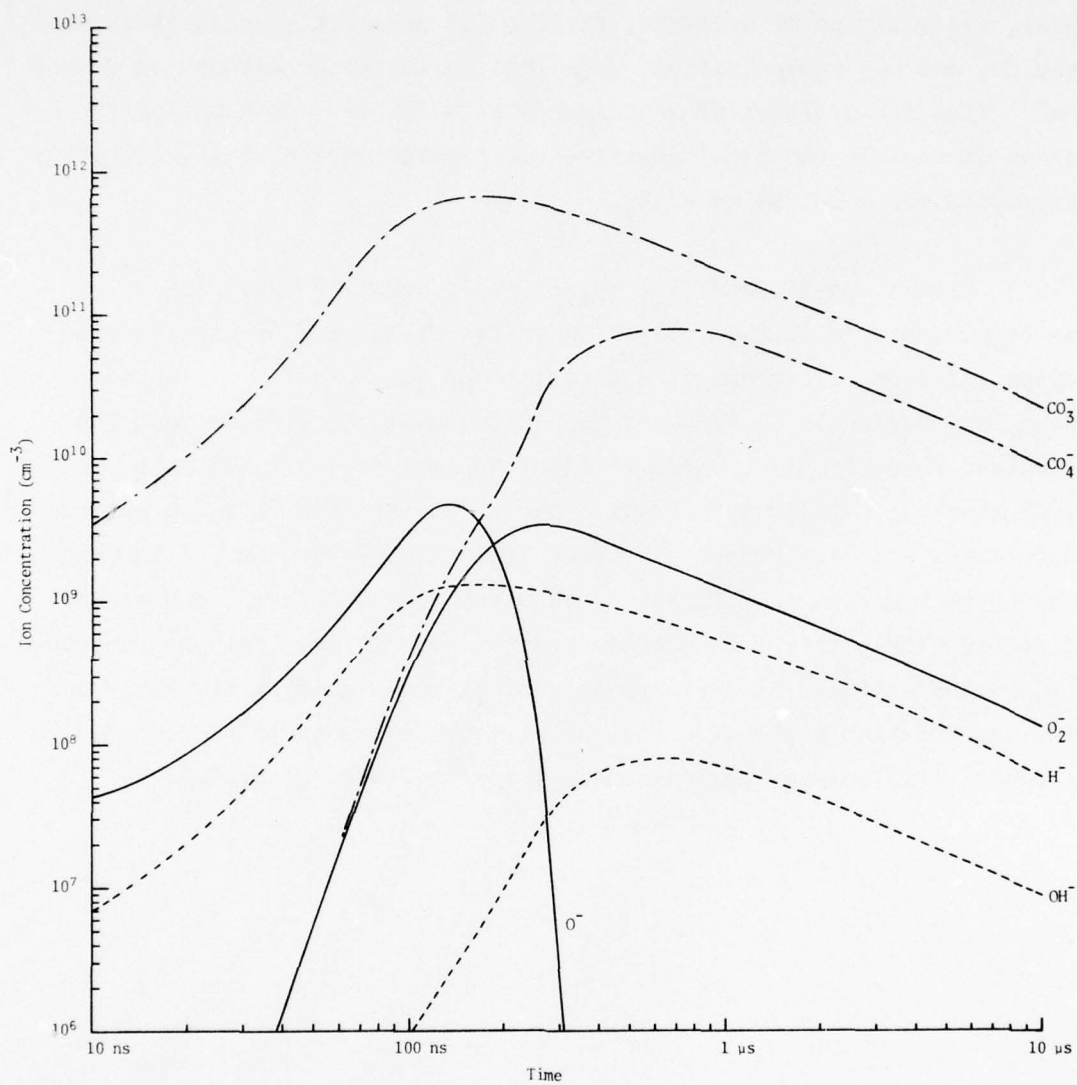


FIGURE 1 - Variation with time of the main negative-ion species in a 70-15-15 He-N<sub>2</sub>-CO<sub>2</sub> mixture.

UNCLASSIFIED

9

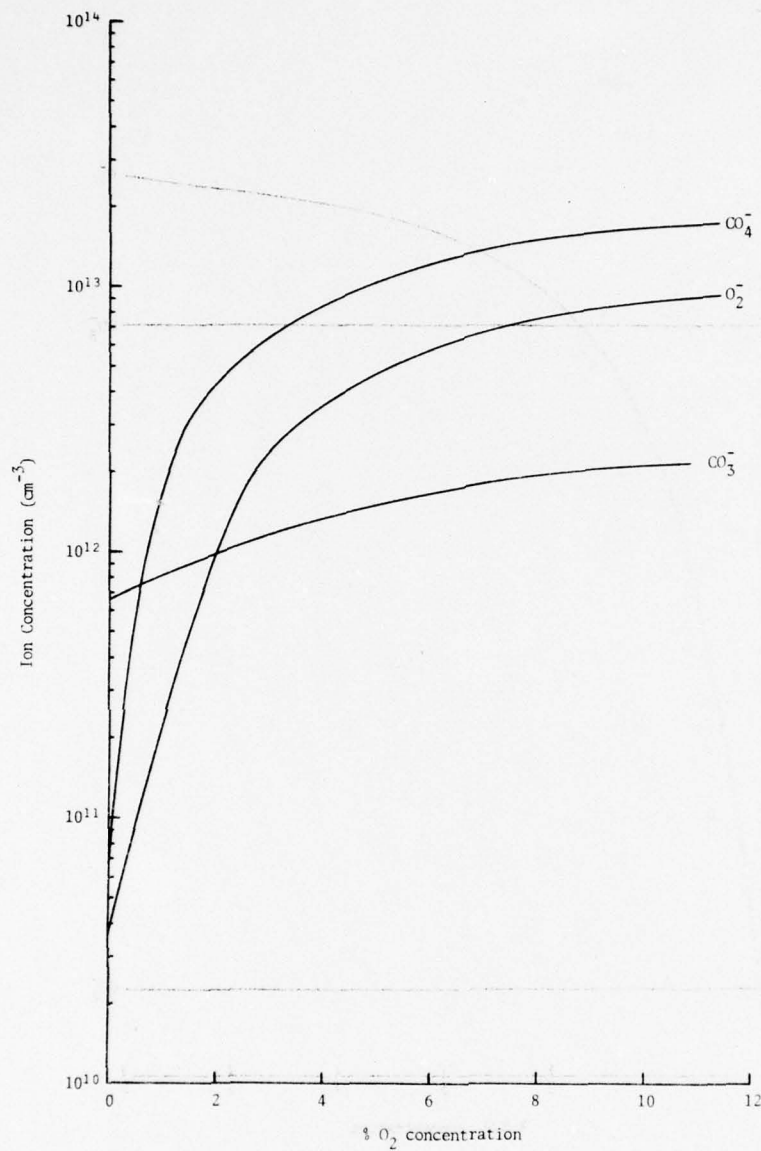


FIGURE 2 - Variation of the main negative-ion concentrations at  $t=150$  ns with various amounts of added oxygen.

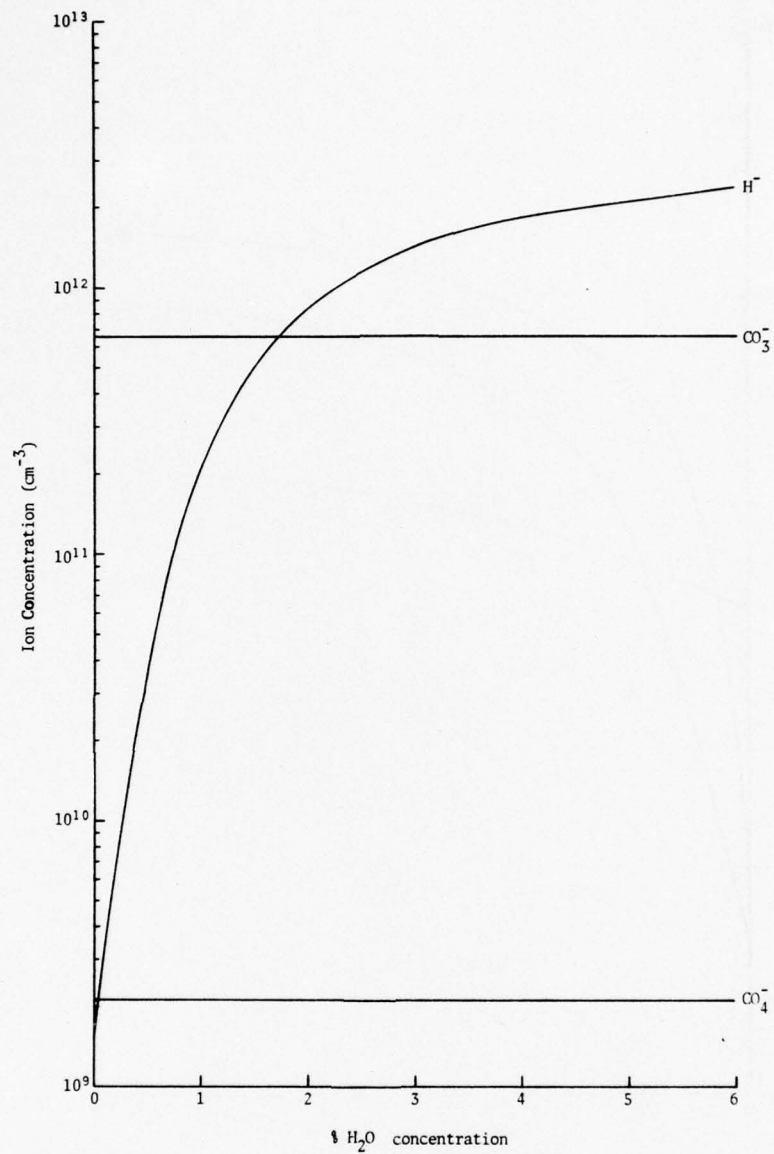


FIGURE 3 - Variation of the main negative-ion concentrations at t=150 ns for various amounts of added water.



### 3.0 COMPARISON WITH EXPERIMENTAL RESULTS

#### 3.1 The High-Repetition-Rate TEA-CO<sub>2</sub> Laser Design

The oscillator module under study employs the double-discharge electrode structure described by Laflamme [4]. The electrode structure consists of a trigger bar, a grid cathode and a solid metallic anode. The trigger bar was wrapped in 12 turns of 'Kapton' (a Dupont polyimide film) and was placed about 1-2 mm behind the grid. The anode was an aluminium plate. In this type of laser the width and length of the discharge are controlled by the trigger bar and thus it is not necessary to shape the electrodes to a uniform-field profile as long as the flat surface of the electrodes is larger than the discharge. However, since it has been shown that uniform pre-ionization normal to the main-discharge electric field is essential in obtaining arc-free discharges [14], a uniform-field-electrode was constructed for the trigger bar [15]. The grid was constructed from a 0.2 mm thick brass sheet perforated with 0.8 mm diameter holes giving a 55-60 percent transmission. The electrodes were arranged to be parallel and uniform to within 0.02 mm. The dimensions of the discharge volume were  $1 \times 1 \times 30 \text{ cm}^3$ .

The gas recirculation system was constructed according to wind-tunnel design considerations presented by Pankurst and Holder [16]. The gas was recirculated by means of seven small fans (Rotron Aximax-1), and cooling was performed by water circulating through the surfaces of the wind-tunnel. The gas flow in the laser was measured using a Pitot-static technique and the results indicate essentially uniform turbulent flow with a velocity of about 20 m/s. According to the analysis of Dzakowic and Wutzke [3], repetition frequencies of about 1000 pulses/s should be attainable. It was not possible to verify this limit as our power supply was only capable of 100 pulses/s operation.

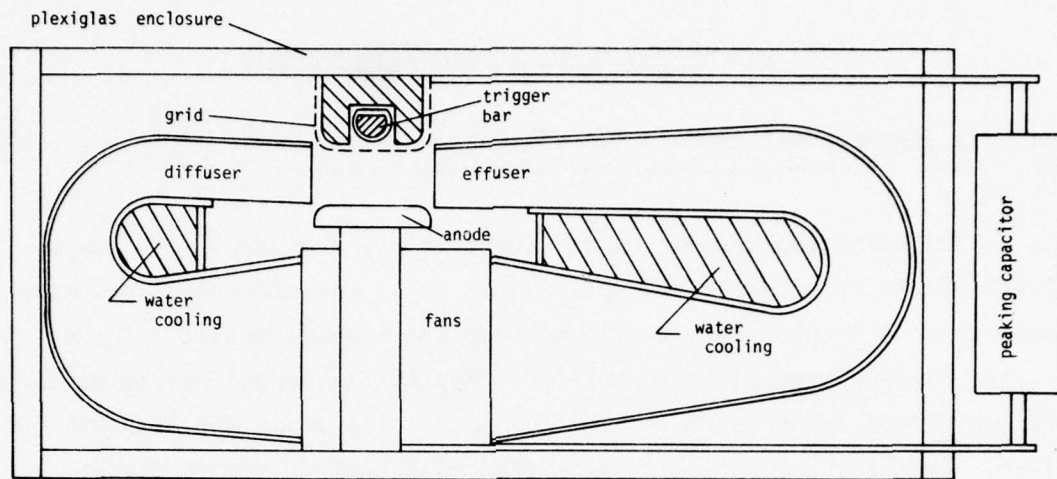


FIGURE 4 - Cross sectional diagram of the laser.

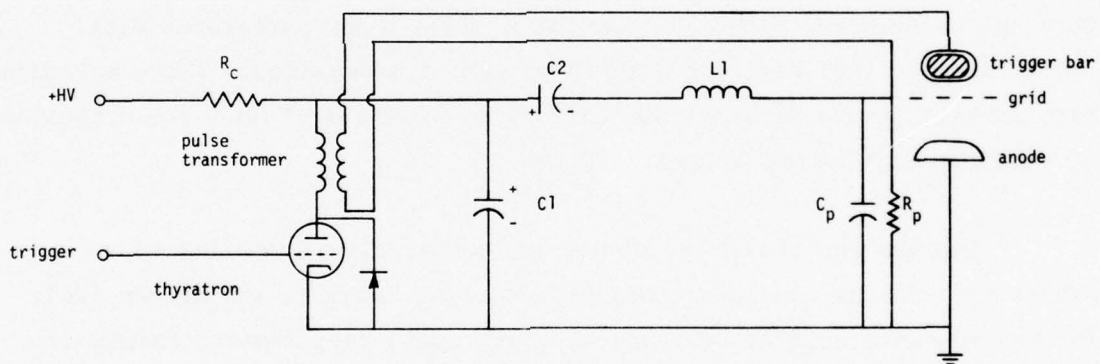


FIGURE 5 - Electrical circuit of the laser  $C_1=0.02 \mu\text{F}$ ,  $C_2=0.01 \mu\text{F}$ ,  
 $C_p=0.01 \mu\text{F}$ ,  $R_p=25 \Omega$ ,  $L_1=10 \mu\text{H}$ .

The laser electrodes and the gas recirculation system were mounted in a Plexiglas box,  $40 \times 20 \times 8 \text{ cm}^3$ , fitted with Brewster-angled NaCl windows. The gas recirculation system was not sealed off from the rest of the box giving a total gas volume of about  $5.6 \text{ l}$ . A schematic diagram of the laser is shown in Fig. 4.

The excitation system for the laser is depicted schematically in Fig. 5. The operation of this circuit has been presented previously [5, 17] and will not be discussed in this report.

### 3.2 Laser Performance

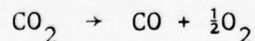
A detailed investigation of this type of laser discharge has already been presented [4, 18]. However, a summary of typical conditions will be given. At an operating input energy density of  $60 \text{ J/l}$  and a 'make-up' gas flow of  $15 \text{ l/min}$ , the discharge and output power remained uniform under continuous operation at  $100 \text{ pulses/s}$  for at least an hour. This type of operation was obtained using a 70% He, 15%  $\text{N}_2$  and 15%  $\text{CO}_2$  gas mixture. The laser was operated with an optical cavity consisting of a totally reflecting 10-metre-radius-of-curvature mirror and a flat partially transmitting output mirror separated from the former by one metre. The pulse shape and output energy can be partially controlled by the output mirror reflectivity as has been shown by Girard and Beaulieu [19]; however, it was found that an 80% reflectivity mirror gave the highest output energies. The peak power of the pulse as measured with a photon drag detector and a Tektronix 556 oscilloscope was about  $1.5 \text{ MW}$  with a total energy of about  $300 \text{ mJ}$ . With an  $8 \text{ mm}$  iris inserted into the cavity, single transverse mode operation produced output energies of about  $120 \text{ mJ/pulse}$  with a peak power of about  $1.0 \text{ MW}$  in a  $60 \text{ ns}$  full-width-half-maximum spike with a pulse risetime of about  $50 \text{ ns}$ , followed by a tail of  $2 \text{ }\mu\text{s}$ . The beam divergence was measured to have a half angle of  $1.5 \pm 0.3 \text{ mrad}$  [20], which is about 1.4 times the diffraction limited value calculated for the resonator configuration used in the experiments [21].

### 3.3 Dissociation in a Sealed TEA-CO<sub>2</sub> Laser

Using the techniques of Stark et al [1], various tests were performed to try and seal the laser. With a standard gas mixture of 70% He, 15% N<sub>2</sub> and 15% CO<sub>2</sub>, it was found that the mean output power (as measured with a CRL model 201 power meter) while operating at 30-40 pulses/s decreased with time until arcing occurred after about 10<sup>4</sup> pulses. In order to try and understand the nature of this effect, we have studied the various laser gas mixtures during and after laser operation using a Micromass partial pressure analyzer. The studies were performed on mixtures containing various proportions of the additives hydrogen and carbon monoxide and the results were compared to the predictions made by the theoretical model.

Since the model predicts that the addition of 1-2% of oxygen will greatly increase the negative-ion population, which leads to arcing, measurements were performed on a standard gas mixture of 70-15-15, He-N<sub>2</sub>-CO<sub>2</sub> to determine the oxygen concentration as a function of the number of pulses. In all cases arcing started to occur when the oxygen concentration had reached about 2%. This can be compared to the computer model where the addition of 2% oxygen causes almost an order of magnitude increase in the negative-ion concentration.

Considering these results and the fact that we have always found the decomposition to obey the equation:



we can use the results of Smith [22] to calculate the dissociation coefficient and thus the rate constant for this reaction. According to Smith and Austin [9], the dissociation of CO<sub>2</sub> in He-N<sub>2</sub>-CO<sub>2</sub> gas mixtures is due to single-electron impact processes. Using this fact, Smith [22] has calculated that the dissociation coefficient is given by:



$$\alpha/P = \frac{0.0057 V}{nE\ell^2 C} \ln \frac{P_n}{P_o} \text{ electron}^{-1} \text{ cm}^{-1} \text{ Torr}^{-1}$$

where  $A\ell$  is the discharge volume,  $V$  is the total gas volume,  $n$  is the number of pulses,  $\ell$  is the discharge gap length,  $E\ell$  is the potential to which the capacitor  $C$  is charged and  $A$  is the discharge cross-sectional area.  $P_o$  and  $P_n$  are the partial pressures of  $\text{CO}_2$  before and after the total number of pulses  $n$ . Fig. 6 is a plot of  $-\ln(P_n/P_o)$  and the number of pulses  $n$ . The results indicate that there is essentially no reformation of  $\text{CO}_2$  up to about 4000 pulses, at which time the concentration of oxygen and  $\text{CO}$  has increased sufficiently to cause some recombination to occur. The graph indicates that an equilibrium dissociation would probably be established. However, after about  $2 \times 10^4$  pulses, the oxygen concentration has increased enough to cause discharge arcing. If we use only the linear portion of the curve, assuming that in this region there is very little recombination, we can calculate a value for  $\alpha/P$  to be about  $6.3 \pm 1.1 \text{ electron}^{-1} \text{ cm}^{-1} \text{ Torr}^{-1}$ . It should be noted that the value of  $\alpha/P$  varies with the discharge electric field and, thus, with the energy injected into the discharge. In order to study this the dissociation coefficient was measured for various values of the energy density injected into the discharge. The results are shown in Fig. 7 for a mixture with 1%  $\text{CO}$  added. It can be seen that  $\alpha/P$  varies linearly with the discharge energy density and under typical operating conditions of  $60 \text{ J}/\ell$  has a value of about  $2\text{--}3 \text{ electron}^{-1} \text{ cm}^{-1} \text{ Torr}^{-1}$ . Under similar operating conditions ( $E = 18 \text{ kV}/\text{cm}$ ) Austin et al [23] have found that for a gas mixture of 4%  $\text{CO}_2$  - 4%  $\text{N}_2$  - 92%  $\text{He}$  the value of  $\alpha/P$  was  $6.7 \pm 1.5 \text{ electron}^{-1} \text{ cm}^{-1} \text{ Torr}^{-1}$  at atmospheric pressure. These values can be compared to the same reduced field values ( $24 \text{ V cm}^{-1} \text{ Torr}^{-1}$ ) for  $\alpha/P$  obtained at lower pressures. Smith and Austin [9] quote a value of  $\alpha/P = 0.35 \pm 0.05 \text{ electron}^{-1} \text{ cm}^{-1} \text{ Torr}^{-1}$  for pure  $\text{CO}_2$  and  $5.5 \pm 0.5 \text{ electron}^{-1} \text{ cm}^{-1} \text{ Torr}^{-1}$  for a 6%  $\text{CO}_2$  - 12%  $\text{N}_2$  - 82%  $\text{He}$  mixture, both with pulsed and continuous discharges. A mixture of 7%  $\text{CO}_2$  - 7%  $\text{N}_2$  - 86%  $\text{He}$  at atmospheric pressure gave an  $\alpha/P$  of  $3.4 \pm 1 \text{ electron}^{-1} \text{ cm}^{-1} \text{ Torr}^{-1}$ .

Obviously the dissociation coefficient depends on the gas mixture and has a value similar to that of a low pressure discharge. It can also be seen that the dissociation coefficient for a mixture is greater than that for pure  $\text{CO}_2$ .

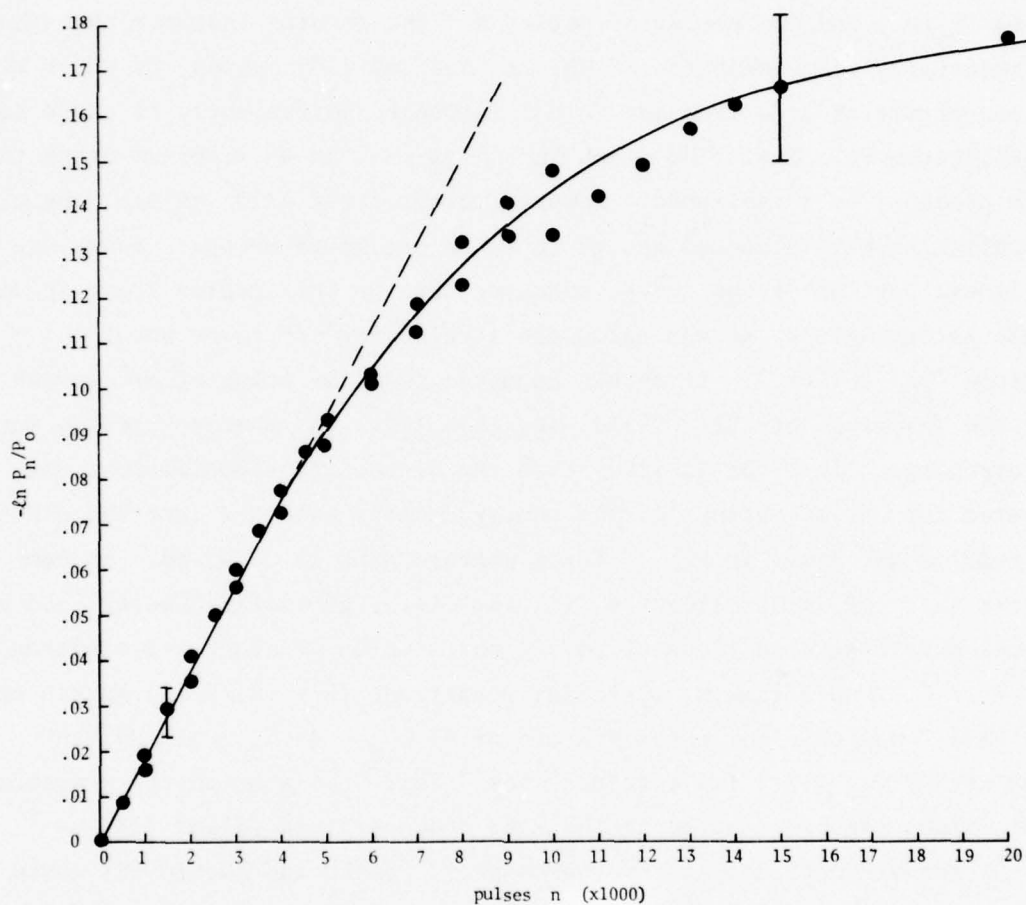


FIGURE 6 - Variation of  $-\ln (P_n/P_o)$  of  $\text{CO}_2$  with number of pulses in a 70-15-15 He- $\text{N}_2$ - $\text{CO}_2$  gas mixture.

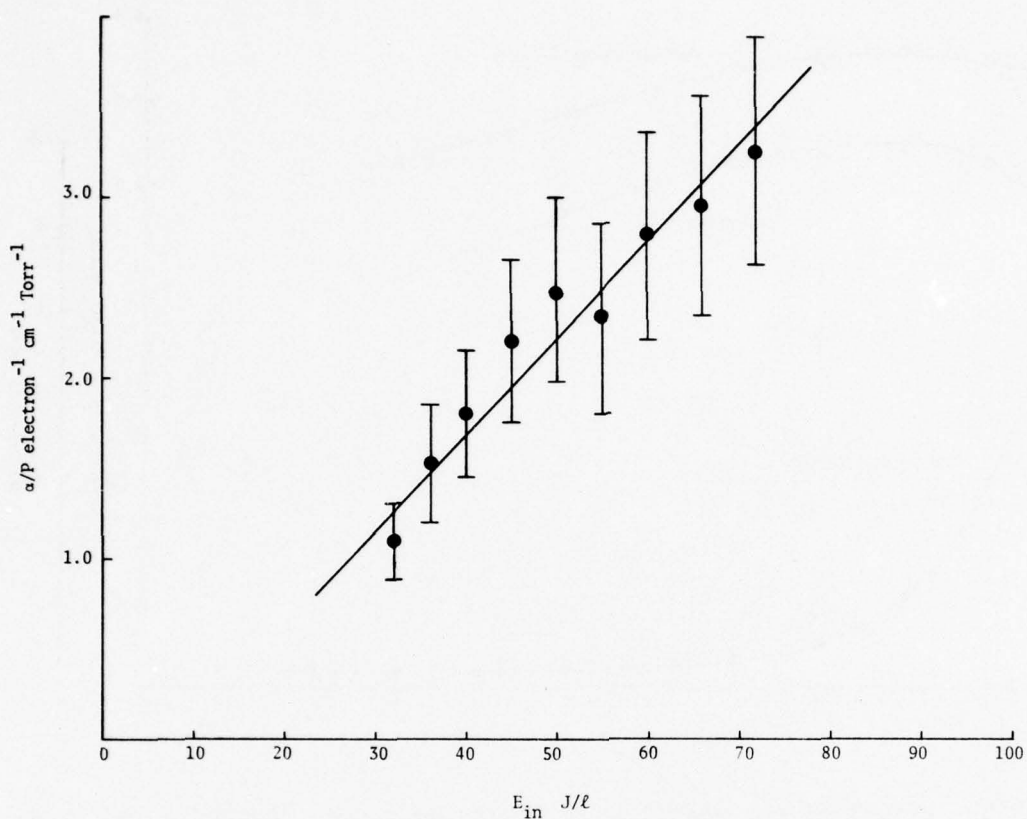


FIGURE 7 - Variation of the dissociation coefficient  $\alpha/P$  with energy injected into the discharge.

#### 3.4 Sealed TEA-CO<sub>2</sub> Laser Operation

We have investigated the effects of the addition of small amounts of CO and hydrogen on the dissociation equilibrium by varying the amounts of each additive separately and measuring the resulting dissociation of a 70-15-15 He-N<sub>2</sub>-CO<sub>2</sub> gas mixture. The tests were performed at a repetition frequency of 30 pulses/s and the resulting dissociation was measured after equilibrium had been established. This was typically 30-40 thousand pulses at an injected energy density of 60 J/l.

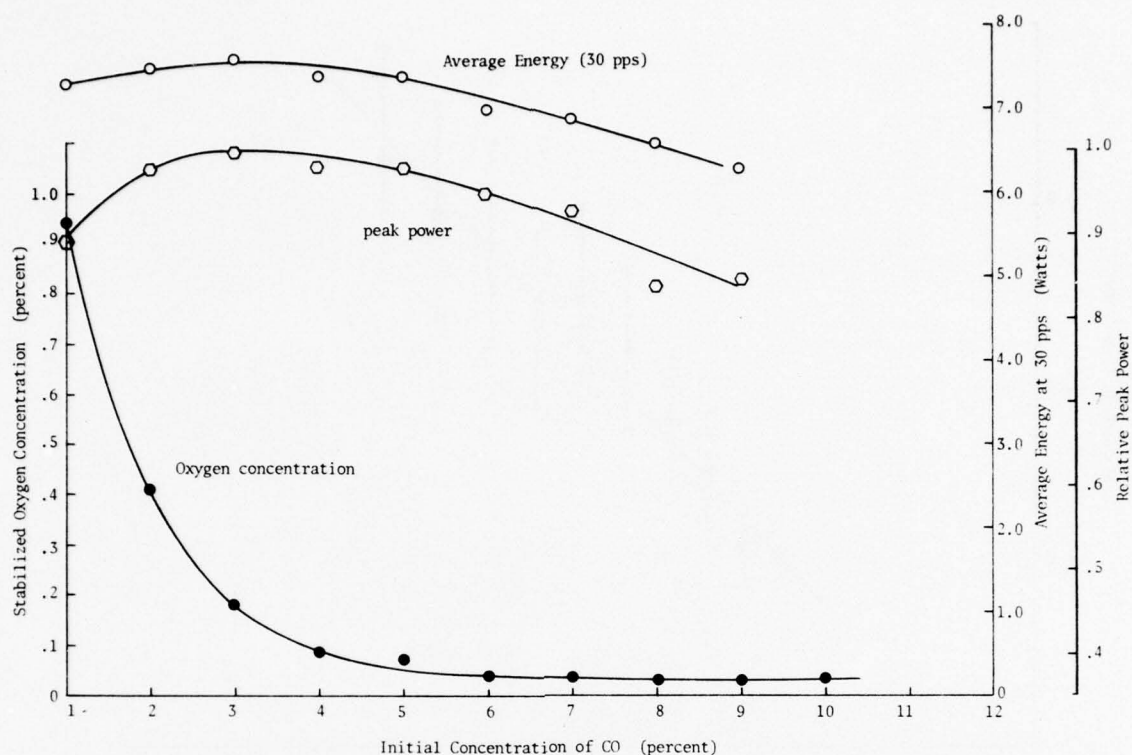


FIGURE 8 - Effect of the addition of CO on the oxygen concentration in a 70-15-15 He-N<sub>2</sub>-CO<sub>2</sub> gas mixture.

The results for the addition of small amounts of CO are presented in Fig. 8. In all cases it was found that about 0.7% of hydrogen was needed to enable stable operation so, in the results presented in Fig. 8, that quantity of hydrogen was added to the gas mixtures. It can be seen that the dissociation equilibrium, here measured by the oxygen concentration, has decreased considerably with 3-4% added CO. On the same graph we have also plotted the average output energy and relative peak power. It can be seen that both these curves are maximized for an addition of about 3-4% CO and then decrease for larger CO concentrations. It can also be seen that the oxygen content does not significantly decrease for higher initial CO concentrations and thus about 4% added CO seems to be optimal under these



conditions. The shape of the energy and power curves can be explained as follows. For low CO concentrations more  $\text{CO}_2$  is decomposed until an equilibrium is established. This will lower the laser output as there is less  $\text{CO}_2$  to participate in the lasing process. In order to increase the CO concentration we have chosen to replace  $\text{N}_2$  with the appropriate amount of CO. This will lead to a less efficient collisional energy transfer to the  $\text{CO}_2$  ( $00^01$ ) upper laser level. This occurs because the rate constant for the transfer of energy from the  $v=1$  level of CO to the upper  $\text{CO}_2$  laser level is a bit smaller than that for  $\text{N}_2$  [24] and, more importantly, the cross section for excitation of the  $v=1$  level for CO is less than that for  $\text{N}_2$  [25] assuming that the electron energies are unaltered by the addition of small amounts of CO.

The addition of hydrogen was also found to reduce the  $\text{CO}_2$  dissociation. Fig. 9 shows the results of the addition of various amounts of deuterium to an initial gas mixture containing 70% He - 15%  $\text{CO}_2$  - 11%  $\text{N}_2$  - 4% CO. The 4% CO content was chosen as it was the value that gave the highest laser power with a reasonably small decomposition. The decomposition of  $\text{CO}_2$  is minimized for values of the hydrogen concentration greater than about 3-4% but the laser power also decreases for these values of the hydrogen concentration. This can be explained by the fact that hydrogen is relatively efficient at depopulating both the  $00^01$  and  $10^00$  laser levels of  $\text{CO}_2$  [26] and thus as the  $\text{H}_2$  concentration is increased we would expect the laser power to decrease. On the other hand, deuterium is less effective at depopulating these levels [26]. To verify this we tried mixtures with varying amounts of  $\text{D}_2$ . We obtained the same results for the decomposition of  $\text{CO}_2$  with  $\text{D}_2$  concentration as compared to  $\text{H}_2$  but we were able to increase the  $\text{D}_2$  concentration to about 2% before the laser power started to decrease. This can be compared to a value of about 0.5-1% for  $\text{H}_2$ . Thus, by the addition of about 2%  $\text{D}_2$  the dissociation equilibrium of  $\text{CO}_2$  can be decreased and the output power can be held at the same value as with a 0.7% hydrogen content.

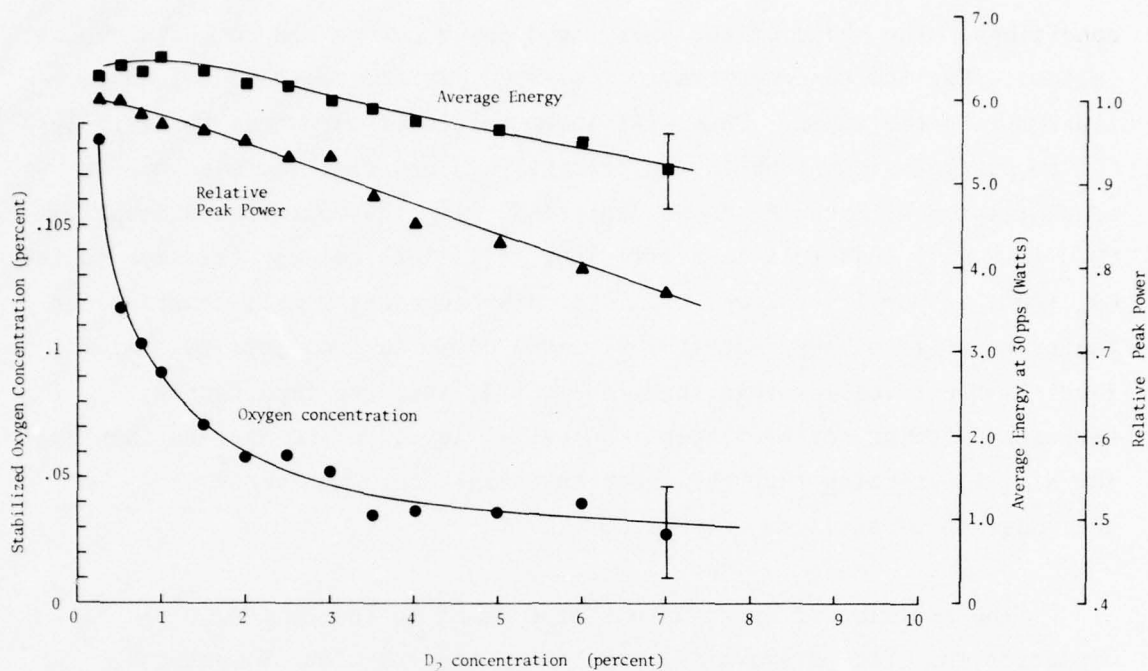
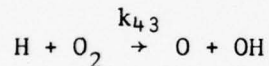


FIGURE 9 - Effect of the addition of  $D_2$  on the oxygen concentration in a 70-11-15-4 He- $N_2$ - $CO_2$ -CO mixture.

However, with the increase in hydrogen/deuterium content the dissociation of hydrogen will lead to considerable amounts of water vapour as a result of the reactions of H and  $H_2$  with other dissociation products, such as O and OH. We can see from Fig. 3 that the addition of about 2-3%  $H_2O$  will double the negative-ion concentration and may lead to discharge arcing. Shields et al [2] have verified the assumption that  $H_2O$  leads to the discharge arcing by passing the laser gases through a water-saturated alumina column before entering the laser and have noted that the discharge arcs. Thus, in this type of discharge it appears that hydrogen has two effects. Firstly, together with CO it limits  $CO_2$  dissociation as discussed in Section 2.2 and secondly, after several pulses  $H_2O$  is formed in the laser. The model predicts that about 2-3% of  $H_2O$  will double the negative-ion concentration by the production of  $H^-$ . Thus, although the first effect of  $H_2$  is beneficial to sealed operation, the second is detrimental and limits the addition of  $H_2$  to small amounts.

### 3.5 Comparison with the Rate Equation Model

In order to compare the results of the rate equation model to the experimental results for the decomposition and reformation of  $\text{CO}_2$ , a series of measurements was made wherein the oxygen concentration was measured as a function of the number of pulses. The results for various gas mixtures are presented in Fig. 10. It can be seen from the figure that an equilibrium state of decomposition is attained for each gas mixture (except the mixture without the CO additive). The number of pulses necessary to obtain this equilibrium depends on the ratio of the discharge volume to the total gas reservoir volume, but in this case equilibrium is attained after 30-40 thousand pulses. As we have used the reaction proposed by Smith and Browne [7] for the reformation of  $\text{CO}_2$ , the reactions involving the production of OH from reactions between hydrogen and oxygen play an important role. In fact, we have found the reformation of  $\text{CO}_2$  very sensitive to the reaction rate for the reaction:



However, there seems to be large discrepancies for the published values of this reaction rate. The value given by Smith and Browne [7] is about  $1.8 \times 10^{-16} \text{ cm}^3 \text{ s}^{-1}$  while the value quoted by Davies et al [6] is about  $9 \times 10^{-18} \text{ cm}^3 \text{ s}^{-1}$ . By using the published values for this reaction rate we were not able to predict the experimentally determined results. It was found necessary to alter the reaction rate in question to a value of about  $1.2 (\pm 0.2) \times 10^{-15} \text{ cm}^3 \text{ s}^{-1}$ .

The results of the computations using this value for the reaction rate are shown in Fig. 10. It can be seen that the equilibrium values for the concentration of oxygen and, thus, the  $\text{CO}_2$  decomposition can be predicted within the bounds of experimental error and the uncertainty in the value of the reaction rate constant  $k_{43}$ . However, the results of the

rate equation model must be treated with caution because many of the rate constants used are not known to better than  $\pm 30\%$ . Nevertheless, the results do indicate that the reactions presented by Smith and Browne do indeed lead to the reformation of  $\text{CO}_2$  from the discharge products and these predictions are verified experimentally.

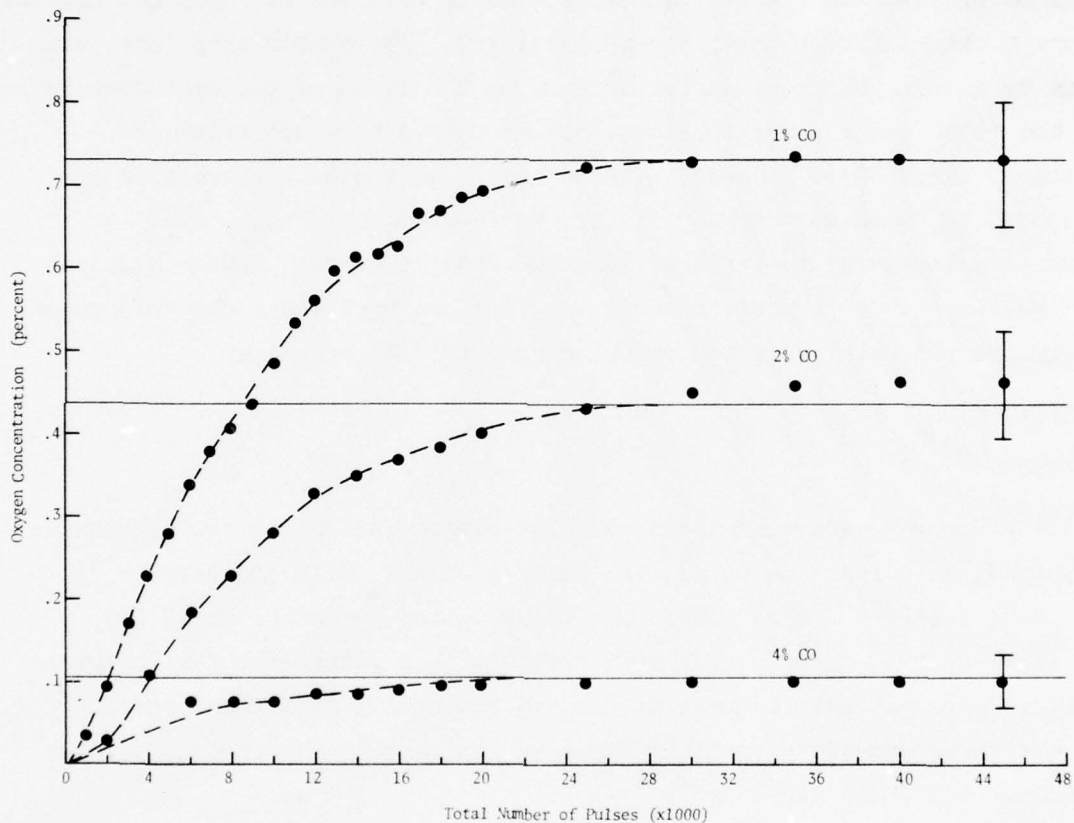


FIGURE 10 - Variation of the oxygen concentration with the number of pulses for mixtures containing various amounts of CO. Equilibrium conditions predicted by the theory are shown as a solid line.



#### 4.0 LONG-LIFE SEALED HIGH-REPETITION-RATE TEA-CO<sub>2</sub> LASER

Finally, to verify the predictions made by the model and the experimental measurements made on the CO<sub>2</sub> decomposition, lifetime tests were performed on a sealed laser operating at repetition frequencies of about 30 pulses/s. Tests were conducted with various initial gas mixtures, but only those mixtures in which the oxygen concentration was predicted to remain less than about 2% were able to maintain arc-free operation. A typical result for a mixture containing He:N<sub>2</sub>:CO<sub>2</sub>:CO:H<sub>2</sub>=69.3:11:15:4:0.7 is shown in Fig. 11. Also shown for comparison is a mixture without CO and hydrogen in the ratio, He:N<sub>2</sub>:CO<sub>2</sub> = 70:15:15. It can be seen that there is an initial power decrease but an equilibrium is attained after about  $2-3 \times 10^4$  pulses. This correlates with the number of pulses required to obtain an equilibrium as measured by the oxygen concentration (as presented in Fig. 10). The tests without the additives indicate that the power continues to decline with the number of pulses and that arcing occurs before an equilibrium state of CO<sub>2</sub> decomposition is attained.

It is not apparent from Fig. 11, but it was observed that the output power declined very gradually with the number of pulses. We also noticed the accumulation of trace amounts of a white powder on the anode. Stark et al [1] have also noticed a similar effect and attributed it to the presence of negative oxygen-bearing ions within the discharge. This would lead to the formation of an oxide layer on the surface of the anode. The presence of negative oxygen-bearing ions is also predicted by the model. This build up of an oxide layer may lead to two possible effects. Firstly, it results in the removal of oxygen from the gas mixture. This would result in more CO<sub>2</sub> decomposing to maintain a certain equilibrium among the CO<sub>2</sub>, CO and oxygen. This loss of CO<sub>2</sub> would cause a decrease in power, as has been seen experimentally. However, we have tested the laser to more than  $2 \times 10^6$  pulses and have noticed only a few percent power decrease after the initial  $3 \times 10^4$  pulses. Secondly, the accumulation of an oxide

layer may bring about a type of Malter effect [27] which would aid in the production of a more uniform discharge. We were not able to verify this assumption; however, it was noticed that the discharge became visually more uniform after the oxide layer had accumulated.

It should be noted that no special care was taken with the vacuum and gas handling systems and the Plexiglas box had an outgassing-leak rate of about  $10 \text{ Pa h}^{-1}$ . Under these conditions we were unable to obtain a shelf-life longer than one week; presumably, this can be improved with better vacuum, materials and techniques. This shelf-life also limited the number of pulses to about  $2 \times 10^6$  as the tests were performed at various intervals during a one-week period.

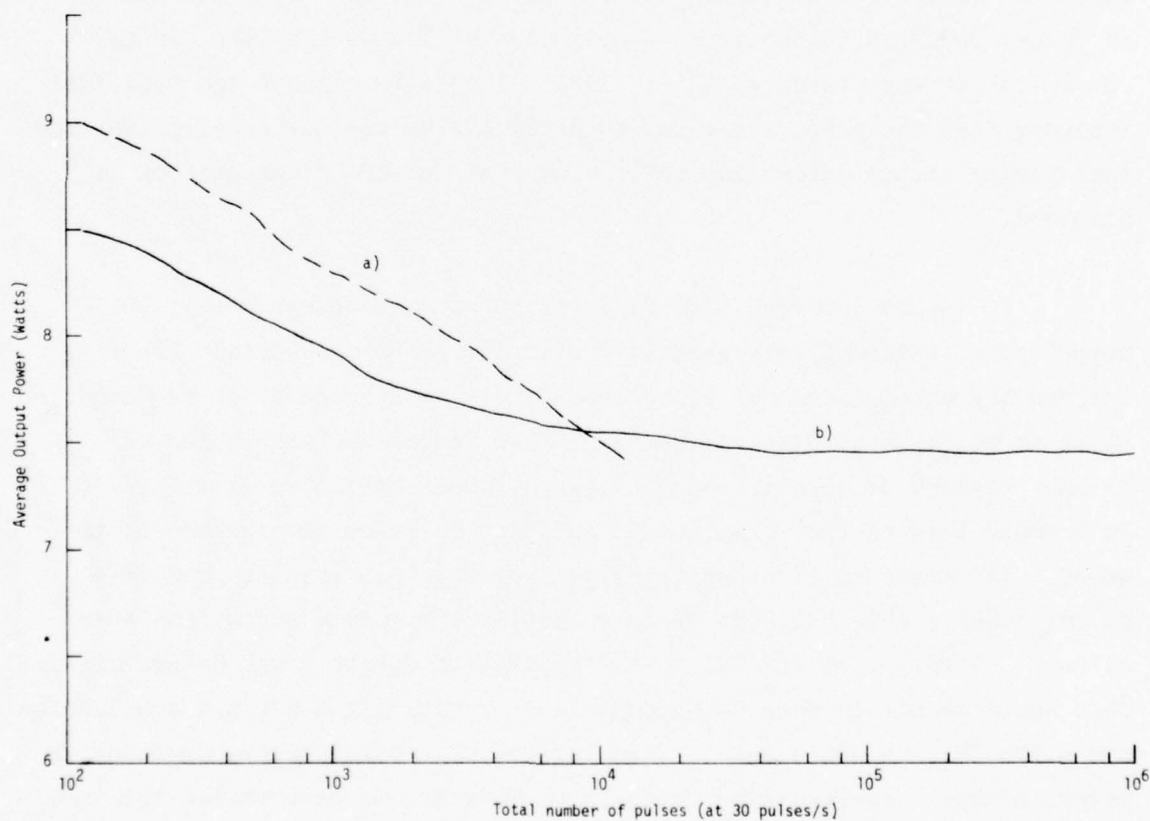


FIGURE 11 - Average output power with number of pulses.

Curve A:  $\text{He:N}_2:\text{CO}_2 = 70:15:15$

Curve B:  $\text{He:N}_2:\text{CO}_2:\text{CO:H}_2 = 69.3:11:15:4:0.7$

## 5.0 CONCLUSIONS

We have demonstrated the operation of a compact high-repetition-rate TEA-CO<sub>2</sub> laser using the double-discharge excitation technique of Laflamme [4]. We have also determined experimentally that sealed laser operation can be obtained in a He-N<sub>2</sub>-CO<sub>2</sub> gas mixture provided that the oxygen concentration remains less than about 1-2%. Theoretically, it has been shown that about 2% O<sub>2</sub> will significantly increase the negative-ion population. Various authors [2, 12] have suggested that discharge instability is due to negative-ion processes which will lead to arcing in TEA-CO<sub>2</sub> lasers. In a sealed system where the discharge products are allowed to accumulate it is found that the dominant negative ion is CO<sub>4</sub><sup>-</sup> and N<sub>n</sub>/N<sub>e</sub> is significantly increased for a mixture with initial concentrations of He:N<sub>2</sub>:CO<sub>2</sub> = 70:15:15. The addition of CO was found to effect the negative-ion population only slightly but along with hydrogen reduced the decomposition of CO<sub>2</sub>. This allows the oxygen concentration to be controlled and thus successful sealed laser operation is possible. However, the addition of hydrogen leads to the production of H<sub>2</sub>O which attaches and produces H<sup>-</sup> in significant quantities.

In order to increase the output energy per pulse one must increase the energy input or the CO<sub>2</sub> concentration. As has been shown, the increase in injected energy will lead to a larger CO<sub>2</sub> dissociation, more oxygen and thus discharge instabilities. A similar effect will occur with additional CO<sub>2</sub> concentrations. Thus, using this method of controlling CO<sub>2</sub> decomposition and this type of laser discharge, it is unlikely that input energy densities much greater than about 60-70 J/ℓ will be realized. However, additional methods to catalyze the reformation of CO<sub>2</sub> from the discharge products (i.e. hot platinum) when combined with the above methods may allow stable operation at higher injected input energy densities, thus allowing higher energy extraction.

UNCLASSIFIED

26

6.0 ACKNOWLEDGEMENTS

The authors would like to acknowledge useful discussions with Dr. G. Kimbell, Dr. R. Stuart and Dr. G. Perrault.

The assistance of Dr. J.-L. Lachambre and Mr. M. Hale is also appreciated.



APPENDIX A

Electron attachment and detachment; negative-ion-molecule reactions; neutral dissociation and recombination processes.

No.	Reaction	Rate constant (300°K)	References
Dissociation attachment			
1.	$e + \text{CO}_2 \rightarrow \text{CO} + \text{O}^-$	$5 \times 10^{-13} \text{ cm}^3 \text{ s}^{-1}$	Nighan and Wiegand [10]†
2.	$e + \text{CO} \rightarrow \text{C} + \text{O}^-$	$3 \times 10^{-14} \text{ cm}^3 \text{ s}^{-1}$	Nighan and Wiegand [10]†
3.	$e + \text{O}_2 \rightarrow \text{O} + \text{O}^-$	$3 \times 10^{-12} \text{ cm}^3 \text{ s}^{-1}$	Nighan and Wiegand [10]†
4.	$e + \text{H}_2\text{O} \rightarrow \text{H}^- + \text{OH}$	$5 \times 10^{-12} \text{ cm}^3 \text{ s}^{-1}$	Nighan and Wiegand [10]†
5.	$e + \text{H}_2 \rightarrow \text{H}^- + \text{H}$	$1 \times 10^{-13} \text{ cm}^3 \text{ s}^{-1}$	Rapp and Briglia [28]
Three-body attachment			
6.	$e + \text{O}_2 + \text{M} \rightarrow \text{O}_2^- + \text{M}$	$2 \times 10^{-30} \text{ cm}^6 \text{ s}^{-1} \text{ (M=O}_2\text{)}$	Phelps [29]
		$1 \times 10^{-31} \text{ cm}^6 \text{ s}^{-1} \text{ (M=N}_2\text{)}$	Phelps [29]
		$3 \times 10^{-30} \text{ cm}^6 \text{ s}^{-1} \text{ (M=CO}_2\text{)}$	Phelps [29]
		$2 \times 10^{-30} \text{ cm}^6 \text{ s}^{-1} \text{ (M=He)}$	Chanin et al [30]
7.	$e + \text{O} + \text{M} \rightarrow \text{O}^- + \text{M}$	$1 \times 10^{-31} \text{ cm}^6 \text{ s}^{-1} \text{ (M=O}_2\text{)}$	Bastien et al [31]
		$1 \times 10^{-31} \text{ cm}^6 \text{ s}^{-1} \text{ (M=N}_2\text{)}$	Bastien et al [31]
Associative detachment			
8.	$\text{O}^- + \text{CO} \rightarrow \text{CO}_2 + e$	$7 \times 10^{-10} \text{ cm}^3 \text{ s}^{-1}$	McFarland et al [32] Moruzzi and Phelps [33]
9.	$\text{O}^- + \text{O} \rightarrow \text{O}_2 + e$	$2 \times 10^{-10} \text{ cm}^3 \text{ s}^{-1}$	Niles [34], Melton [35]
10.	$\text{O}^- + \text{O}_2(^1\Delta_g) \rightarrow \text{O}_3 + e$	$1 \times 10^{-10} \text{ cm}^3 \text{ s}^{-1}$	Niles [34]
11.	$\text{O}^- + \text{H}_2 \rightarrow \text{H}_2\text{O} + e$	$8 \times 10^{-10} \text{ cm}^3 \text{ s}^{-1}$	Phelps [29]
12.	$\text{CO}_3^- + \text{CO} \rightarrow 2\text{CO}_2 + e$	$5 \times 10^{-13} \text{ cm}^3 \text{ s}^{-1}$	Shields et al [2]
13.	$\text{O}_2^- + \text{O} \rightarrow \text{O}_3 + e$	$3 \times 10^{-10} \text{ cm}^3 \text{ s}^{-1}$	Niles [34], Melton [35]

## UNCLASSIFIED

28

No.	Reaction	Rate constant (300°K)	References
14.	$O_2^- + O_2(^1\Delta_g) \rightarrow 2O_2 + e$	$2 \times 10^{-10} \text{ cm}^3 \text{ s}^{-1}$	Fehsenfeld et al [36]
15.	$O_2^- + H \rightarrow HO_2 + e$	$1 \times 10^{-9} \text{ cm}^3 \text{ s}^{-1}$	Fehsenfeld [37]
16.	$H^- + H \rightarrow H_2 + e$	$1 \times 10^{-9} \text{ cm}^3 \text{ s}^{-1}$	McDaniel et al [38]
17.	$H^- + O_2 \rightarrow HO_2 + e$	$1 \times 10^{-9} \text{ cm}^3 \text{ s}^{-1}$	McDaniel et al [38]
18.	$OH^- + O \rightarrow HO_2 + e$	$2 \times 10^{-10} \text{ cm}^3 \text{ s}^{-1}$	Melton [35]
19.	$OH^- + H \rightarrow H_2O + e$	$1 \times 10^{-9} \text{ cm}^3 \text{ s}^{-1}$	Melton [35]
Neutral dissociation			
20.	$e + CO_2 \rightarrow CO + O + e$	$0.5 \times 10^{-9} \text{ cm}^3 \text{ s}^{-1}$	Present work Smith and Austin [9]
21.	$e + O_2 \rightarrow O + O + e$	$1 \times 10^{-9} \text{ cm}^3 \text{ s}^{-1}$	see text
22.	$e + H_2 \rightarrow H + H + e$	$4 \times 10^{-9} \text{ cm}^3 \text{ s}^{-1}$	see text
23.	$e + H_2O \rightarrow H + OH + e$	$2 \times 10^{-9} \text{ cm}^3 \text{ s}^{-1}$	see text
Neutral recombination			
24.	$O + CO + M \rightarrow CO_2 + M$	$2 \times 10^{-36} \text{ cm}^6 \text{ s}^{-1}$	Stuhl and Niki [37]
25.	$O + O + M \rightarrow O_2 + M$	$3 \times 10^{-33} \text{ cm}^6 \text{ s}^{-1}$	Niles [34]
26.	$O + O_2 + M \rightarrow O_3 + M$	$5 \times 10^{-34} \text{ cm}^6 \text{ s}^{-1}$	Niles [34]
27.	$O + O_3 \rightarrow O_2 + O_2$	$9 \times 10^{-15} \text{ cm}^3 \text{ s}^{-1}$	Niles [34]
28.	$H + H + M \rightarrow H_2 + M$	$8.4 \times 10^{-33} \text{ cm}^6 \text{ s}^{-1}$	Davies et al [6]
Negative-ion-molecule two-body reactions			
29.	$O^- + O_2(^1\Delta_g) \rightarrow O_2^- + O$	$1 \times 10^{-9} \text{ cm}^3 \text{ s}^{-1}$	Niles [34]
30.	$O^- + H_2 \rightarrow OH^- + H$	$3 \times 10^{-11} \text{ cm}^3 \text{ s}^{-1}$	McFarland et al [32]
31.	$O_2^- + O \rightarrow O_2 + O^-$	$1 \times 10^{-11} \text{ cm}^3 \text{ s}^{-1}$	Niles [34]
32.	$O_2^- + O_3 \rightarrow O_2 + O_3^-$	$4 \times 10^{-10} \text{ cm}^3 \text{ s}^{-1}$	Niles [34], Melton [35]
33.	$O_2^- + H \rightarrow H^- + O_2$	$2 \times 10^{-9} \text{ cm}^3 \text{ s}^{-1}$	Fehsenfeld [38]
34.	$CO_3^- + O \rightarrow O_2^- + CO_2$	$8 \times 10^{-11} \text{ cm}^3 \text{ s}^{-1}$	Niles [34], Melton [35]

No.	Reaction	Rate constant (300°K)	References
35.	$\text{CO}_3^- + \text{H} \rightarrow \text{OH}^- + \text{CO}_2$	$2 \times 10^{-10} \text{ cm}^3 \text{ s}^{-1}$	Fehsenfeld [37]
36.	$\text{CO}_4^- + \text{O} \rightarrow \text{CO}_3^- + \text{O}_2$	$2 \times 10^{-10} \text{ cm}^3 \text{ s}^{-1}$	McDaniel et al [39]
37.	$\text{CO}_4^- + \text{O}_3 \rightarrow \text{O}_3^- + \text{CO}_2 + \text{O}_2$	$1 \times 10^{-10} \text{ cm}^3 \text{ s}^{-1}$	Bastien et al [31] Fehsenfeld and Ferguson [40]
38.	$\text{CO}_4^- + \text{H} \rightarrow \text{CO}_3^- + \text{OH}$	$2 \times 10^{-10} \text{ cm}^3 \text{ s}^{-1}$	Fehsenfeld [38]
Negative-ion-molecule three-body reactions			
39.	$\text{O}^- + \text{CO}_2 + \text{M} \rightarrow \text{CO}_3^- + \text{M}$	$9 \times 10^{-29} \text{ cm}^6 \text{ s}^{-1} \text{ (M=CO}_2\text{)}$ $2 \times 10^{-28} \text{ cm}^6 \text{ s}^{-1} \text{ (M=H}_e\text{)}$ $3 \times 10^{-28} \text{ cm}^6 \text{ s}^{-1} \text{ (M=O}_2\text{)}$	Moruzzi and Phelps [33] Fehsenfeld and Ferguson [40] Fehsenfeld and Ferguson [40]
40.	$\text{O}_2^- + \text{CO}_2 + \text{M} \rightarrow \text{CO}_4^- + \text{M}$	$1 \times 10^{-29} \text{ cm}^6 \text{ s}^{-1} \text{ (M=CO}_2\text{)}$ $1 \times 10^{-29} \text{ cm}^6 \text{ s}^{-1} \text{ (M=O}_2\text{)}$ $5 \times 10^{-29} \text{ cm}^6 \text{ s}^{-1} \text{ (M=O}_2\text{)}$	Melton [35] Melton [35] Fehsenfeld and Ferguson [40]
Neutral two-body reactions			
41.	$\text{O} + \text{OH} \rightarrow \text{O}_2 + \text{H}$	$3.3 \times 10^{-11} \text{ cm}^3 \text{ s}^{-1}$	Smith and Browne [7] Davies et al [6]
42.	$\text{H}_2 + \text{O} \rightarrow \text{H} + \text{OH}$	$1 \times 10^{-14} \text{ cm}^3 \text{ s}^{-1}$	Smith and Browne [7]
43.	$\text{H} + \text{O}_2 \rightarrow \text{O} + \text{OH}$	$1.2 \times 10^{-15} \text{ cm}^3 \text{ s}^{-1}$	see text
44.	$\text{H} + \text{OH} \rightarrow \text{H}_2 + \text{O}$	$3.5 \times 10^{-17} \text{ cm}^3 \text{ s}^{-1}$	Davies et al [6]
45.	$\text{H}_2 + \text{OH} \rightarrow \text{H}_2\text{O} + \text{H}$	$6.5 \times 10^{-15} \text{ cm}^3 \text{ s}^{-1}$	Smith and Browne [7]
46.	$\text{H}_2\text{O} + \text{H} \rightarrow \text{H}_2 + \text{OH}$	$2 \times 10^{-25} \text{ cm}^3 \text{ s}^{-1}$	Davies et al [6]
47.	$\text{H}_2\text{O} + \text{O} \rightarrow \text{OH} + \text{OH}$	$5 \times 10^{-24} \text{ cm}^3 \text{ s}^{-1}$	Davies et al [6]
48.	$\text{OH} + \text{OH} \rightarrow \text{H}_2\text{O} + \text{O}$	$2.4 \times 10^{-13} \text{ cm}^3 \text{ s}^{-1}$	Smith and Browne [7]
49.	$\text{H} + \text{HO}_2 \rightarrow \text{OH} + \text{OH}$	$1.7 \times 10^{-11} \text{ cm}^3 \text{ s}^{-1}$	Davies et al [6]
50.	$\text{OH} + \text{OH} \rightarrow \text{H} + \text{HO}_2$	$1 \times 10^{-40} \text{ cm}^3 \text{ s}^{-1}$	Davies et al [6]
51.	$\text{H} + \text{HO}_2 \rightarrow \text{H}_2 + \text{O}_2$	$1.3 \times 10^{-11} \text{ cm}^3 \text{ s}^{-1}$	Davies et al [6]

## UNCLASSIFIED

30

No.	Reaction	Rate constant (300°K)	References
52.	$\text{H}_2 + \text{O}_2 \rightarrow \text{H} + \text{HO}_2$	$7 \times 10^{-53} \text{ cm}^3 \text{ s}^{-1}$	Davies et al [6]
53.	$\text{H}_2\text{O}_2 + \text{OH} \rightarrow \text{H}_2\text{O} + \text{HO}_2$	$8 \times 10^{-13} \text{ cm}^3 \text{ s}^{-1}$	Davies et al [6]
54.	$\text{H}_2\text{O} + \text{HO}_2 \rightarrow \text{H}_2\text{O}_2 + \text{OH}$	$6 \times 10^{-35} \text{ cm}^3 \text{ s}^{-1}$	Davies et al [6]
55.	$\text{H}_2\text{O}_2 + \text{H} \rightarrow \text{H}_2 + \text{HO}_2$	$5 \times 10^{-15} \text{ cm}^3 \text{ s}^{-1}$	Davies et al [6]
56.	$\text{H}_2 + \text{HO}_2 \rightarrow \text{H}_2\text{O}_2 + \text{H}$	$3 \times 10^{-26} \text{ cm}^3 \text{ s}^{-1}$	Davies et al [6]
57.	$\text{HO}_2 + \text{CO} \rightarrow \text{CO}_2 + \text{OH}$	$1.5 \times 10^{-27} \text{ cm}^3 \text{ s}^{-1}$	Davies et al [6]
58.	$\text{O} + \text{CO} \rightarrow \text{CO}_2 + h\nu$	$2 \times 10^{-20} \text{ cm}^3 \text{ s}^{-1}$	Davies et al [6]
59.	$\text{OH} + \text{CO} \rightarrow \text{CO}_2 + \text{H}$	$1.5 \times 10^{-13} \text{ cm}^3 \text{ s}^{-1}$	Smith and Browne [7]
60.	$\text{O} + \text{HO}_2 \rightarrow \text{OH} + \text{O}_2$	$9 \times 10^{-12} \text{ cm}^3 \text{ s}^{-1}$	Davies et al [6]

† For a mean electron energy of 1 eV

Rates with a known temperature dependence have been quoted at 300°K.



APPENDIX B

Following is a summary of the rate equations used to describe the time dependence of the various negative-ion and neutral species. The rate coefficients are denoted by  $k$  with a numerical subscript referring to the appropriate reaction as listed in Appendix A.  $n_e$  is the electron density,  $n_p$  is the positive ion density, which in this case is equal to the total number of negative charges as we have assumed charge neutrality, and  $F$  is the fraction of molecular oxygen in the ( $^1\Delta_g$ ) state.  $k_{2R}$  and  $k_{3R}$  are the two-body and the three-body negative-ion-positive-ion recombination rates.

$$\begin{aligned} \frac{d[CO_3^-]}{dt} &= k_{39}[O^-][CO_2][M] + k_{36}[CO_4^-][O] + k_{38}[CO_4^-][H] \\ &- (k_{12}[CO] + k_{34}[CO] + k_{35}[H] + k_{2R}n_p + k_{3R}[M]n_p) [CO_3^-] \end{aligned}$$

$$\begin{aligned} \frac{d[O^-]}{dt} &= n_e (k_1[CO_2] + k_2[CO] + k_3[O_2] + k_7[O][M]) \\ &+ k_{31}[O_2^-][O] - (k_{39}[CO_2][M] + k_8[CO] + k_9[O] \\ &+ k_{10}F[O_2] + k_{29}F[O_2] + k_{30}[H_2] + k_{11}[H_2] \\ &+ k_{2R}n_p + k_{3R}[M]n_p) [O^-] \end{aligned}$$

$$\begin{aligned} \frac{d[O_2^-]}{dt} &= n_e k_6[O_2][M] + k_{29}F[O_2] + k_{34}[CO_3^-][O] \\ &- (k_{13}[O] + k_{14}F[O_2] + k_{15}[H] + k_{31}[O] + k_{32}[O_3] \\ &+ k_{33}[H] + k_{40}[CO_2][M] + k_{2R}n_p + k_{3R}[M]n_p) [O_2^-] \end{aligned}$$

$$\begin{aligned} \frac{d[CO_4^-]}{dt} &= k_{40}[O_2^-][CO_2][M] - (k_{36}[O] + k_{37}[O_3] \\ &+ k_{38}[H] + k_{2R}n_p + k_{3R}[M]n_p) [CO_4^-] \end{aligned}$$

$$\begin{aligned} \frac{d[H^-]}{dt} &= n_e (k_4[H_2O] + k_5[H_2]) + k_{33}[O_2^-][H] \\ &- (k_{16}[H] + k_{17}[O_2] + k_{2R}n_p + k_{3R}[M]n_p) [H^-] \end{aligned}$$

$$\begin{aligned}
\frac{d[H]}{dt} = & n_e (k_5[H_2] + 2k_{28}[H_2] + k_{23}[H_2O] + k_{30}[O^-][H_2] \\
& + k_{41}[O][OH] + k_{42}[H_2][O] + k_{45}[H_2][OH] + k_{50}[OH][OH] \\
& + k_{52}[H_2][O_2] + k_{56}[H_2][HO_2] + k_{59}[OH][CO_2] \\
& - (k_{15}[O_2^-] + k_{16}[H^-] + k_{19}[OH^-] + k_{33}[O_2^-] + k_{35}[CO_3^-] \\
& + k_{38}[CO_4^-] + k_{28}[H][M] + k_{43}[O_2] + k_{44}[OH] \\
& + k_{46}[H_2O] + k_{49}[HO_2] + k_{51}[HC_2] + k_{55}[H_2O_2]) [H]
\end{aligned}$$

$$\begin{aligned}
\frac{d[H_2]}{dt} = & k_{16}[H^-][H] + k_{28}[H][H][M]/2 + k_{44}[H][OH] \\
& + k_{46}[H_2O][H] + k_{51}[H][HO_2] + k_{55}[H_2O_2][H] \\
& - (n_e k_5 + k_{11}[O^-] + k_{22}n_e + k_{30}[O^-] + k_{42}[O] \\
& + k_{45}[OH] + k_{52}[O_2] + k_{56}[HO_2]) [H_2]
\end{aligned}$$

$$\begin{aligned}
\frac{d[OH^-]}{dt} = & k_{30}[O^-][H_2] + k_{35}[CO_3^-][H] - (k_{18}[O] + k_{19}[H] \\
& + k_{2R}n_p + k_{3R}[M]n_p) [OH^-]
\end{aligned}$$

$$\begin{aligned}
\frac{d[CO]}{dt} = & k_{11}n_e [CO_2] + k_{20}n_e [CO_2] - (k_{21}n_e + k_8[O^-] \\
& + k_{12}[CO_3^-] + k_{24}[O][M] + k_{57}[HO_2] + k_{58}[O] \\
& + k_{59}[OH]) [CO]
\end{aligned}$$

$$\begin{aligned}
\frac{d[O]}{dt} = & n_e (k_3[O_2] + k_{20}[CO_2] + 2k_{21}[O_2]) + k_{35}^F[O^-][O_2] \\
& + k_{43}[H][O_2] + k_{44}[H][OH] + k_{48}[OH][OH] - (k_7n_e[M] \\
& + k_9[O^-] + k_{13}[O_2^-] + k_{18}[OH^-] + k_{24}[CO][M] \\
& + k_{25}[O][M] + k_{26}[O_2][M] + k_{27}[O_3] + k_{31}[O_2^-] \\
& + k_{34}[CO_3^-] + k_{36}[CO_4^-] + k_{41}[OH] + k_{42}[H_2] \\
& + k_{47}[H_2O] + k_{58}[CO] + k_{60}[HO_2]) [O]
\end{aligned}$$

$$\begin{aligned}
\frac{d[O_2]}{dt} = & k_9[O^-][O] + 2k_{14}[O_2^-]F[O_2] + k_{25}[O][O][M] + 2k_{27}[O][O_3] \\
& + k_{31}[O_2^-][O] + k_{32}[O_2^-][O_3] + k_{33}[O_2^-][H] + k_{36}[CO_4^-][O] \\
& + k_{37}[CO_4^-][O_3] + k_{41}[O][OH] + k_{51}[H][HO_2] + k_{60}[O][HO_2] \\
& - (k_3n_e + k_6n_e[M] + k_{21}n_e + k_{26}[O][M] \\
& + k_{43}[H] + k_{52}[H_2] + k_{17}[H^-]) [O_2]
\end{aligned}$$

$$\begin{aligned}
\frac{d[O_3]}{dt} = & k_{10}[O^-]F[O_2] + k_{13}[O_2^-][O] + k_{26}[O][O_2][M] \\
& - (k_{27}[O] + k_{32}[O_2^-] + k_{37}[CO_4^-]) [O_3]
\end{aligned}$$

$$\begin{aligned}
\frac{d[CO_2]}{dt} = & k_8[O^-][CO] + 2k_{12}[CO_3^-][CO] + k_{24}[O][CO][M] \\
& + k_{34}[CO_3^-][O] + k_{35}[CO_3^-][H] + k_{37}[CO_4^-][O_3] \\
& + k_{57}[HO_2][CO] + k_{58}[O][CO] + k_{59}[OH][CO] \\
& - (k_1n_e + k_{20}n_e + k_{39}[O^-][M] + k_{40}[O_2^-][M]) [CO_2]
\end{aligned}$$

$$\begin{aligned}
\frac{d[H_2O]}{dt} = & k_{11}[O^-][H_2] + k_{19}[OH^-][H] + k_{45}[H_2][OH] \\
& + k_{48}[OH][OH] + k_{53}[H_2O_2][OH] - (k_4n_e + k_{23}n_e \\
& + k_{46}[H] + k_{47}[O] + k_{54}[HO_2]) [H_2O]
\end{aligned}$$

$$\begin{aligned}
\frac{d[OH]}{dt} = & k_4n_e[H_2O] + k_{23}n_e[H_2O] + k_{38}[CO_4^-][H] \\
& + k_{42}[H_2][O] + k_{43}[H][O_2] + k_{46}[H_2O][H] \\
& + 2k_{47}[H_2O][O] + 2k_{49}[H][HO_2] + k_{54}[H_2O][HO_2] \\
& + k_{57}[HO_2][CO] - (k_{41}[O] + k_{44}[H] + k_{45}[H_2] \\
& + k_{48}[OH] + k_{50}[OH] + k_{53}[H_2O_2] + k_{59}[CO]) [OH]
\end{aligned}$$

$$\begin{aligned}
\frac{d[\text{HO}_2]}{dt} = & k_{15}[\text{O}_2^-][\text{H}] + k_{17}[\text{H}^-][\text{O}_2] + k_{18}[\text{OH}^-][\text{O}] \\
& + k_{50}[\text{OH}][\text{OH}] + k_{52}[\text{H}_2][\text{O}_2] + k_{53}[\text{H}_2\text{O}_2][\text{OH}] \\
& + k_{55}[\text{H}_2\text{O}_2][\text{H}] - (k_{49}[\text{H}] + k_{51}[\text{H}] + k_{56}[\text{H}_2] \\
& + k_{57}[\text{CO}] + k_{60}[\text{O}] + k_{54}[\text{H}_2\text{O}]) [\text{HO}_2]
\end{aligned}$$

$$\begin{aligned}
\frac{d[\text{H}_2\text{O}_2]}{dt} = & k_{54}[\text{H}_2\text{O}][\text{HO}_2] + k_{56}[\text{H}_2][\text{HO}_2] - (k_{53}[\text{OH}] \\
& + k_{55}[\text{H}]) [\text{H}_2\text{O}_2]
\end{aligned}$$



## 7.0 REFERENCES

1. Stark D.S., Cross P.H. and Foster H. 1975, "A compact sealed pulsed CO<sub>2</sub> TEA laser", IEEE J.Q.E., QE-11, 774-78.
2. Shields H., Smith A.L.S. and Norris B. 1976, "Negative ion effects in TEA-CO<sub>2</sub> lasers", J. Phys. D: Appl. Phys., 9, 1587-1603.
3. Dzakowic G.S. and Wutzke S.A. 1973, "High-pulse-rate-glow-discharge stabilization by gas flow", J. Appl. Optics, 44, 5061-63.
4. Laflamme A.K. 1970, "Double-discharge excitation for atmospheric pressure CO<sub>2</sub> lasers", Rev. Sci. Instr., 41, 1578-81.
5. Pace P.W. and Lacombe M. 1977, "A compact high-repetition-rate TEA-CO<sub>2</sub> laser", J. Phys. E. Sci. Instrum., 10, 208-10.
6. Davies A.R., Roberts S.A., Smith K. and Thomson R.M. 1975, "Theoretical modelling of CO<sub>2</sub> lasers", Annual Report to SERL on Project RU-11-8, University of Leeds. UNCLASSIFIED
7. Smith A.L.S. and Browne P.G. 1974, "Catalysis in sealed CO<sub>2</sub> lasers", J. Phys. D: Appl. Phys., 7, 1652-59.
8. Wiederhold G. and Donnerhacke K.H. 1976, "Excitation of CO<sub>2</sub> TEA lasers with self-sustained discharges", Sov. J. Quant. Electron, 6, 474-6.
9. Smith A.L.S. and Austin J.M. 1974, "Dissociation mechanism in pulsed and continuous CO<sub>2</sub> lasers", J. Phys. D: Appl. Phys., 7, 314-22.
10. Nighan W.L. and Wiegand W.J. 1974, "Influence of negative-ion processes on steady-state properties and striations in molecular gas discharges" Phys. Rev. A., 110, 922-45.
11. Johns T.W. and Nation J.A. 1972, "Ionization instability in atmospheric-pressure gas discharges", Appl. Phys. Lett., 20, 495-6.
12. Douglas-Hamilton D.A. and Mani S.A. 1973, "An electron attachment plasma instability", Appl. Phys. Lett., 23, 508-10.
13. Douglas-Hamilton D.A. and Mani S.A. 1974, "Attachment instability in an externally ionized discharge", J. Appl. Phys., 45, 4406-15.
14. Kline L.E. and Denes L.J. 1975, "Investigations of glow discharge formation with volume preionization", J. Appl. Phys., 46, 1567-74.
15. Chang T.Y. 1973, "Improved uniform-field electrode profiles for TEA laser and high-voltage applications", Rev. Sci. Instrum., 44, 405-7.

16. Pankurst R.C. and Holder D.W. 1952, Wind Tunnel Technique (London: Pitman)
17. Lacombe M., Noel M., Blanchard M. and Rheault F. 1975, "Circuits améliorés pour l'excitation de lasers à double décharge", DREV Report 2129/75. NON CLASSIFIE
18. Lachambre J.L., Gilbert J., Rheault F., Fortin R. and Blanchard M. 1973, "Performance characteristics of a TEA double-discharge grid amplifier", IEEE J.Q. Elec., QE-9, 459-68.
19. Girard A and Beaulieu J.A. 1974, "A TEA-CO<sub>2</sub> laser with output pulse length adjustable from 5  $\mu$ s to over 50  $\mu$ s", IEEE J. Q. Elec., QE-10, 521-24.
20. Bergman T.G. 1973, "Measuring divergence with a focusing lens", Laser Focus, 9, 58.
21. Kogelnik H. and Li T. 1966, "Laser beams and resonators", Proc. IEEE, 54, 1312-29.
22. Smith A.L.S. 1975, "Effects of sparks in TEA lasers", J. Phys. D: Appl. Phys., 8, 1387-91.
23. Austin J.M., Smith A.L.S. and Browne P.G. 1974, "Dissociation in TEA-CO<sub>2</sub> lasers", Physics Lett. 46A, 427-428.
24. Hamilton D.D. 1976, "Pulse stretching with CO in a TEA-CO<sub>2</sub> lasers", Optics Commun., 19, 339-42.
25. Shultz G.J. 1964, "Vibrational excitation of N<sub>2</sub>, CO and H<sub>2</sub> by electron impact", Phys. Rev., 135, A988-94.
26. Stricker J. 1966, "Deactivation of CO<sub>2</sub> (010) and CO<sub>2</sub> (001) by hydrogen and deuterium", J. Chem. Phys., 64, 1261-65.
27. Wood O.R., Smith P.W., Adams C.R. and Maloney 1975, "Excitation of transversely excited CO<sub>2</sub> waveguide lasers", Appl. Phys. Lett., 27, 539-41.
28. Rapp D. and Briglia D.D. 1965, "Total cross sections for ionization at attachment in gases by electron impact. II. Negative-ion formation", J. Chem. Phys., 43, 1480-9.
29. Phelps A.V. 1969, "Laboratory studies of electron attachment and detachment processes of aeronomic interest", Can. J. Chem., 47, 1783-93.
30. Chanin L.M., Phelps A.V. and Biondi M.A. 1962, "Measurements of the attachment of low-energy electrons to oxygen molecules", Phys. Rev., 128, 219-30.

31. Bastien F., Haug R. and Lecuiller M. 1975, "Simulation sur ordinateur de l'évolution temporelle des ions négatifs de l'air. Application au cas de la décharge couronne négative", J. Chim. Phys., 72, 105-12.
32. McFarland M., Albritton D.L., Fehsenfeld F.C., Ferguson E.E. and Schmeltekoph A.L. 1973, "Flow-drift technique for ion mobility and ion-molecule reaction rate constant measurements. III Negative ion reactions of  $O^-$  with  $CO$ ,  $NO$ ,  $H_2$  and  $D_2$ ", J. Chem. Phys., 59, 6629-35.
33. Moruzzi J.L. and Phelps A.V. 1966, "Survey of negative-ion-molecule reactions in  $O_2$ ,  $CO_2$ ,  $H_2O$ ,  $CO$  and mixtures of these gases at high pressures", J. Chem. Phys., 45, 4617-27.
34. Niles F.E. 1970, "Airlike discharges with  $CO_2$ ,  $NO$ ,  $NO_2$  and  $N_2O$  impurities", J. Chem. Phys., 52, 408-24.
35. Melton C.E. 1970, Principles of mass spectrometry and negative ions (New-York: Wiley).
36. Fehsenfeld F.C., Ferguson E.E. and Schmeltekoph A.L. 1966, "Thermal-energy associate-detachment reactions of negative ions", J. Chem. Phys., 45, 1844-5.
37. Stuhl F. and Niki H. 1971, "Measurements of rate constants for termolecular reactions of  $O(^3P)$  with  $NO$ ,  $O_2$ ,  $CO$ ,  $N_2$  and  $CO_2$  using a pulsed vacuum-uv photolysis-chemiluminescent method", J. Chem. Phys., 55, 3943-53.
38. Fehsenfeld F.C. 1975, "Reaction of  $CO_3^-$ ,  $NO_3^-$  and  $CO_4^-$ , with atomic hydrogen", J. Chem. Phys., 64, 1686-7.
39. McDaniel E.W., Cermak V., Dalgarno A., Ferguson E.E. and Friedman L. 1970, Ion-molecule reactions (New-York: Wiley).
40. Fehsenfeld F.C. and Ferguson E.E. 1974, "Laboratory studies of negative-ion reactions with atmospheric trace constituents", J. Chem. Phys., 61, 3181-93.



CRDV R-4092/78 (UNCLASSIFIED)

Bureau - Recherche et Développement, Ministère de la Défense nationale, Canada.  
CRDV, C.P. 880, Courcellette, Qué. G0A 1R0.

"A Sealed High-Repetition-Rate TIA-CO<sub>2</sub> Laser"  
by P. Pace and M. Lacombe

Nous avons construit un laser CO<sub>2</sub> TIA à double décharge de petites dimensions et l'avons fait fonctionner à cadence moyenne. L'addition de petites quantités d'hydrogène et de monoxyde de carbone au mélange gazeux He-CO<sub>2</sub>-N<sub>2</sub> nous a permis d'obtenir plus de 2x10<sup>6</sup> impulsions en circuit fermé. Dans ces conditions, l'énergie de sortie atteint environ 250 mJ/impulsion lorsque la cadence est de 40 à 50 Hz.

Dans le but de mieux comprendre les différents processus en jeu dans un laser scellé, nous avons analysé le mélange gazeux à l'aide d'un spectromètre de masse.

A la suite de ces analyses, nous avons trouvé qu'il est possible de faire fonctionner un laser en circuit fermé pourvu que la concentration de l'oxygène présente dans le mélange gazeux He-CO<sub>2</sub>-N<sub>2</sub>-CO-H<sub>2</sub> demeure inférieure à 1-2 pour cent. Nous avons ensuite comparé nos résultats aux prédictions tirées d'un modèle théorique qui tient compte des processus mettant en jeu les particules neutres et les ions négatifs. Ces calculs nous montrent que la présence de faibles quantités d'oxygène et d'eau dans le milieu gazeux fait augmenter le nombre d'ions négatifs produits dans la décharge au point que le rapport ions négatifs à électrons, N<sub>-</sub>/N<sub>e</sub>, peut se rapprocher de l'unité. Le modèle indique également que des quantités adéquates d'hydrogène/deutérium et de monoxyde de carbone peuvent servir à contrôler la dissociation du CO<sub>2</sub>. (NC)

CRDV R-4092/78 (UNCLASSIFIED)

Bureau - Recherche et Développement, Ministère de la Défense nationale, Canada.  
CRDV, C.P. 880, Courcellette, Qué. G0A 1R0.

"A Sealed High-Repetition-Rate TIA-CO<sub>2</sub> Laser"  
by P. Pace and M. Lacombe

Nous avons construit un laser CO<sub>2</sub> TIA à double décharge de petites dimensions et l'avons fait fonctionner à cadence moyenne. L'addition de petites quantités d'hydrogène et de monoxyde de carbone au mélange gazeux He-CO<sub>2</sub>-N<sub>2</sub> nous a permis d'obtenir plus de 2x10<sup>6</sup> impulsions en circuit fermé. Dans ces conditions, l'énergie de sortie atteint environ 250 mJ/impulsion lorsque la cadence est de 40 à 50 Hz.

Dans le but de mieux comprendre les différents processus en jeu dans un laser

scellé, nous avons analysé le mélange gazeux à l'aide d'un spectromètre de masse. A la suite de ces analyses, nous avons trouvé qu'il est possible de faire fonctionner un laser en circuit fermé pourvu que la concentration de l'oxygène présente dans le mélange gazeux He-CO<sub>2</sub>-N<sub>2</sub>-CO-H<sub>2</sub> demeure inférieure à 1-2 pour cent. Nous avons ensuite comparé nos résultats aux prédictions tirées d'un modèle théorique qui tient compte des processus mettant en jeu les particules neutres et les ions négatifs. Ces calculs nous montrent que la présence de faibles quantités d'oxygène et d'eau dans le milieu gazeux fait augmenter le nombre d'ions négatifs produits dans la décharge au point que le rapport ions négatifs à électrons, N<sub>-</sub>/N<sub>e</sub>, peut se rapprocher de l'unité. Le modèle indique également que des quantités adéquates d'hydrogène/deutérium et de monoxyde de carbone peuvent servir à contrôler la dissociation du CO<sub>2</sub>. (NC)

CRDV R-4092/78 (UNCLASSIFIED)

Bureau - Recherche et Développement, Ministère de la Défense nationale, Canada.  
CRDV, C.P. 880, Courcellette, Qué. G0A 1R0.

"A Sealed High-Repetition-Rate TIA-CO<sub>2</sub> Laser"  
by P. Pace and M. Lacombe

Nous avons construit un laser CO<sub>2</sub> TIA à double décharge de petites dimensions et l'avons fait fonctionner à cadence moyenne. L'addition de petites quantités d'hydrogène et de monoxyde de carbone au mélange gazeux He-CO<sub>2</sub>-N<sub>2</sub> nous a permis d'obtenir plus de 2x10<sup>6</sup> impulsions en circuit fermé. Dans ces conditions, l'énergie de sortie atteint environ 250 mJ/impulsion lorsque la cadence est de 40 à 50 Hz.

Dans le but de mieux comprendre les différents processus en jeu dans un laser scellé, nous avons analysé le mélange gazeux à l'aide d'un spectromètre de masse.

A la suite de ces analyses, nous avons trouvé qu'il est possible de faire fonctionner un laser en circuit fermé pourvu que la concentration de l'oxygène présente dans le mélange gazeux He-CO<sub>2</sub>-N<sub>2</sub>-CO-H<sub>2</sub> demeure inférieure à 1-2 pour cent. Nous avons ensuite comparé nos résultats aux prédictions tirées d'un modèle théorique qui tient compte des processus mettant en jeu les particules neutres et les ions négatifs. Ces calculs nous montrent que la présence de faibles quantités d'oxygène et d'eau dans le milieu gazeux fait augmenter le nombre d'ions négatifs produits dans la décharge au point que le rapport ions négatifs à électrons, N<sub>-</sub>/N<sub>e</sub>, peut se rapprocher de l'unité. Le modèle indique également que des quantités adéquates d'hydrogène/deutérium et de monoxyde de carbone peuvent servir à contrôler la dissociation du CO<sub>2</sub>. (NC)

CRDV R-4092/78 (UNCLASSIFIED)

Bureau - Recherche et Développement, Ministère de la Défense nationale, Canada.  
CRDV, C.P. 880, Courcellette, Qué. G0A 1R0.

"A Sealed High-Repetition-Rate TIA-CO<sub>2</sub> Laser"  
by P. Pace and M. Lacombe

Nous avons construit un laser CO<sub>2</sub> TIA à double décharge de petites dimensions et l'avons fait fonctionner à cadence moyenne. L'addition de petites quantités d'hydrogène et de monoxyde de carbone au mélange gazeux He-CO<sub>2</sub>-N<sub>2</sub> nous a permis d'obtenir plus de 2x10<sup>6</sup> impulsions en circuit fermé. Dans ces conditions, l'énergie de sortie atteint environ 250 mJ/impulsion lorsque la cadence est de 40 à 50 Hz.

Dans le but de mieux comprendre les différents processus en jeu dans un laser

scellé, nous avons analysé le mélange gazeux à l'aide d'un spectromètre de masse. A la suite de ces analyses, nous avons trouvé qu'il est possible de faire fonctionner un laser en circuit fermé pourvu que la concentration de l'oxygène présente dans le mélange gazeux He-CO<sub>2</sub>-N<sub>2</sub>-CO-H<sub>2</sub> demeure inférieure à 1-2 pour cent. Nous avons ensuite comparé nos résultats aux prédictions tirées d'un modèle théorique qui tient compte des processus mettant en jeu les particules neutres et les ions négatifs. Ces calculs nous montrent que la présence de faibles quantités d'oxygène et d'eau dans le milieu gazeux fait augmenter le nombre d'ions négatifs produits dans la décharge au point que le rapport ions négatifs à électrons, N<sub>-</sub>/N<sub>e</sub>, peut se rapprocher de l'unité. Le modèle indique également que des quantités adéquates d'hydrogène/deutérium et de monoxyde de carbone peuvent servir à contrôler la dissociation du CO<sub>2</sub>. (NC)



DREV R-4092/78 (UNCLASSIFIED)

Research and Development Branch, Department of National Defence, Canada,  
DREV, P.O. Box 880, Courcellette, Que. G0A 1R0

"A Sealed High-Repetition-Rate TEA-CO<sub>2</sub> Laser"  
by P. Pace and M. Lacombe

A compact atmospheric pressure CO<sub>2</sub> laser utilizing a double-discharge technique has been constructed and operated at moderate repetition rates. With the addition of small amounts of hydrogen and carbon monoxide to the He-CO<sub>2</sub>-N<sub>2</sub> gas mixture, sealed operational lifetimes exceeding 2x10<sup>6</sup> pulses have been obtained. Operating in this mode, the output energy is about 250 mJ/pulse at repetition frequencies of 40-50 pulses/s.

In order to better understand the processes involved in the operation of a sealed laser, we have performed mass spectroscopic measurements of the laser gas mixture. It has been determined that sealed operation is possible as long as oxygen concentration below 1-2 percent in a He-CO<sub>2</sub>-N<sub>2</sub>-CO-H<sub>2</sub> gas mixture is maintained. Experimental results are compared to the predictions of a theoretical model in which neutral and negative-ion processes have been included. The calculations indicate that, when small amounts of oxygen or water are present in the discharge, the negative-ion population is significantly increased and the ratio of negative-ions to electrons N<sub>-</sub>/N<sub>e</sub> can approach values near unity. The model also predicts that the dissociation equilibrium of the CO<sub>2</sub> can be controlled by the addition of the appropriate amounts of hydrogen/deuterium and carbon monoxide. (U)

DREV R-4092/78 (UNCLASSIFIED)

Research and Development Branch, Department of National Defence, Canada,  
DREV, P.O. Box 880, Courcellette, Que. G0A 1R0

"A Sealed High-Repetition-Rate TEA-CO<sub>2</sub> Laser"  
by P. Pace and M. Lacombe

A compact atmospheric pressure CO<sub>2</sub> laser utilizing a double-discharge technique has been constructed and operated at moderate repetition rates. With the addition of small amounts of hydrogen and carbon monoxide to the He-CO<sub>2</sub>-N<sub>2</sub> gas mixture, sealed operational lifetimes exceeding 2x10<sup>6</sup> pulses have been obtained. Operating in this mode, the output energy is about 250 mJ/pulse at repetition frequencies of 40-50 pulses/s.

In order to better understand the processes involved in the operation of a sealed laser, we have performed mass spectroscopic measurements of the laser gas mixture. It has been determined that sealed operation is possible as long as oxygen concentration below 1-2 percent in a He-CO<sub>2</sub>-N<sub>2</sub>-CO-H<sub>2</sub> gas mixture is maintained. Experimental results are compared to the predictions of a theoretical model in which neutral and negative-ion processes have been included. The calculations indicate that, when small amounts of oxygen or water are present in the discharge, the negative-ion population is significantly increased and the ratio of negative-ions to electrons N<sub>-</sub>/N<sub>e</sub> can approach values near unity. The model also predicts that the dissociation equilibrium of the CO<sub>2</sub> can be controlled by the addition of the appropriate amounts of hydrogen/deuterium and carbon monoxide. (U)

DREV R-4092/78 (UNCLASSIFIED)

Research and Development Branch, Department of National Defence, Canada,  
DREV, P.O. Box 880, Courcellette, Que. G0A 1R0

"A Sealed High-Repetition-Rate TEA-CO<sub>2</sub> Laser"  
by P. Pace and M. Lacombe

A compact atmospheric pressure CO<sub>2</sub> laser utilizing a double-discharge technique has been constructed and operated at moderate repetition rates. With the addition of small amounts of hydrogen and carbon monoxide to the He-CO<sub>2</sub>-N<sub>2</sub> gas mixture, sealed operational lifetimes exceeding 2x10<sup>6</sup> pulses have been obtained. Operating in this mode, the output energy is about 250 mJ/pulse at repetition frequencies of 40-50 pulses/s.

In order to better understand the processes involved in the operation of a sealed laser, we have performed mass spectroscopic measurements of the laser gas mixture. It has been determined that sealed operation is possible as long as oxygen concentration below 1-2 percent in a He-CO<sub>2</sub>-N<sub>2</sub>-CO-H<sub>2</sub> gas mixture is maintained. Experimental results are compared to the predictions of a theoretical model in which neutral and negative-ion processes have been included. The calculations indicate that, when small amounts of oxygen or water are present in the discharge, the negative-ion population is significantly increased and the ratio of negative-ions to electrons N<sub>-</sub>/N<sub>e</sub> can approach values near unity. The model also predicts that the dissociation equilibrium of the CO<sub>2</sub> can be controlled by the addition of the appropriate amounts of hydrogen/deuterium and carbon monoxide. (U)

DREV R-4092/78 (UNCLASSIFIED)

Research and Development Branch, Department of National Defence, Canada,  
DREV, P.O. Box 880, Courcellette, Que. G0A 1R0

"A Sealed High-Repetition-Rate TEA-CO<sub>2</sub> Laser"  
by P. Pace and M. Lacombe

A compact atmospheric pressure CO<sub>2</sub> laser utilizing a double-discharge technique has been constructed and operated at moderate repetition rates. With the addition of small amounts of hydrogen and carbon monoxide to the He-CO<sub>2</sub>-N<sub>2</sub> gas mixture, sealed operational lifetimes exceeding 2x10<sup>6</sup> pulses have been obtained. Operating in this mode, the output energy is about 250 mJ/pulse at repetition frequencies of 40-50 pulses/s.

In order to better understand the processes involved in the operation of a sealed laser, we have performed mass spectroscopic measurements of the laser gas mixture. It has been determined that sealed operation is possible as long as oxygen concentration below 1-2 percent in a He-CO<sub>2</sub>-N<sub>2</sub>-CO-H<sub>2</sub> gas mixture is maintained. Experimental results are compared to the predictions of a theoretical model in which neutral and negative-ion processes have been included. The calculations indicate that, when small amounts of oxygen or water are present in the discharge, the negative-ion population is significantly increased and the ratio of negative-ions to electrons N<sub>-</sub>/N<sub>e</sub> can approach values near unity. The model also predicts that the dissociation equilibrium of the CO<sub>2</sub> can be controlled by the addition of the appropriate amounts of hydrogen/deuterium and carbon monoxide. (U)